Elsevier Editorial System(tm) for Chemical Engineering Science
Manuscript Draft

Manuscript Number:

Title: Adsorption of Propane, Propylene and Isobutane on a Metal-organic Framework: Molecular Simulation and Experiment

Article Type: Regular Article

Section/Category:

Keywords: Adsorption; Separations; Olefin/paraffin; Porous Media; Metal-organic frameworks; Molecular Simulation

Corresponding Author: Dr. Miguel Jorge, Ph.D.

Corresponding Author's Institution: Faculty of Engineering, University of Porto

First Author: Nabil Lamia

Order of Authors: Nabil Lamia; Miguel Jorge, Ph.D.; Miguel A Granato; Filipe A Paz; Hubert Chevreau; Alirio E Rodrigues

Manuscript Region of Origin:

Abstract: The separation of propane/propylene mixtures is the most energy-intensive operation practiced in the petrochemical industry. Adsorptive processes are currently viewed as a promising alternative to cryogenic distillation for the separation of these mixtures. In this paper, we explore the possibility of using a new metal-organic framework material, CuBTC, in adsorptive separation processes, particularly in a simulated moving bed (SMB) context using isobutane as a potential desorbent. A gravimetric method has been used to measure the adsorption equilibrium isotherms of propylene, propane and isobutane onto a commercial CuBTC powder over a temperature range from 323 K to 423 K and pressures up to 100 kPa. These were complemented by a detailed

experimental characterization of the structure of CuBTC using XRD and SEM techniques. Comparison of experimental isotherms with grand canonical Monte Carlo simulations in CuBTC showed that propane adsorption occurs preferentially in small octahedral pockets, while isobutane is excluded from these pockets due to its bulky structure. Propylene was seen to interact strongly with unsaturated metal sites, due to specific π-Cu bonds. These interactions significantly enhance the affinity of this MOF for unsaturated hydrocarbons. Furthermore, in a range of temperatures and pressures, the affinity of CuBTC for isobutane is intermediate to that of propane and propylene. Our results suggest that CuBTC-isobutane is a very promising adsorbent-desorbent pair for use in SMB processes for propane/propylene separations.

To the Editor of Chemical Engineering Science.

Dear Sir,

Please find attached the manuscript entitled "**Adsorption of Propane, Propylene and Isobutane on a Metal-organic Framework: Molecular Simulation and Experiment**", by Nabil Lamia, Miguel Jorge, Miguel A. Granato, Filipe A. A. Paz, Hubert Chevreau and Alírio E. Rodrigues. We hope it can be considered for publication in *Chem. Eng. Sci.* as an Article.

In this manuscript, we report detailed adsorption measurements of propane, propylene and isobutane in CuBTC, a metal-organic framework (MOF) material. MOFs constitute a recent and exciting development in porous material technology, showing promising properties for gas storage and separations. However, their high potential has not yet been translated into effective improvements in separation process technology. This paper represents a step in this direction, and aims to develop an understanding of the adsorption process of alkanes and alkenes in MOFs. For that purpose, we adopt a strategy that combines careful experimental adsorption studies and material characterization with molecular simulation methods. This approach has enabled us to shed new light on the adsorption mechanism of propane, propylene and isobutane in CuBTC. Furthermore, we have assessed the suitability of using this material in a simulated moving bed process for olefin/paraffin separations, using isobutane as a desorbent. We believe our study will help bridge the gap between the molecular and the process level, and will strongly contribute to the incorporation of MOFs in industrial adsorptive separation processes.

Contact details of the corresponding author:
Miguel Jorge
LSRE – Laboratory of Separation and Reaction Engineering
Faculdade de Engenharia da Universidade do Porto
Rua Dr. Roberto Frias, s/n
4200-465 Porto
Portugal
Phone: +351 225081686
Fax: +351 225081674
email: mjorge@fe.up.pt

*** Reviewer Suggestions**

Suggested Reviewers:

1) Duong D. Do
Department of Chemical Engineering
The University of Queensland
St Lucia, Brisbane
Qld 4072, Australia
Phone: (61) 7 3365 4154
Fax: (61) 7 3365 2789
email: duongd@cheque.uq.edu.au

2) Tina Duren
School of Engineering and Electronics
University of Edinburgh
Mayfield Road, Edinburgh
UK
email: Tina.Duren@ed.ac.uk
Phone: +44 (0)131 6504856
Fax: +44 (0)131 6506551

3) Jose Antonio Delgado
Department of Chemical Engineering,
Universidad Complutense de Madrid,
Spain
email: jadeldob@quim.ucm.es

4) Randall Snurr
Department of Chemical Engineering
Northwestern University
2145 Sheridan Road E136
Evanston, IL 60208
USA
Tel. 1-847-467-2977
Fax 1-847-467-1018
email: snurr@northwestern.edu

5) Daniel Tondeur
Laboratoire des Sciences du Génie Chimique,
CNRS-ENSIC-INPL
1, Rue Grandville, BP 451,
F-54001 Nancy cedex,
France
Tel: +33 3 83 17 51 90
Fax: +33 3 83 32 29 75
email: Daniel.Tondeur@ensic.inpl-nancy.fr

6) Peter A. Monson
Chemical Engineering Department
University of Massachusetts Amherst
686 N. Pleasant Street
Amherst, MA 01003-9303
USA
tel: +1-413-545-0661
fax: +1-413-545-1647
email: monson@ecs.umass.edu

Adsorption of Propane, Propylene and Isobutane on a Metal-organic Framework: Molecular Simulation and Experiment

Nabil LAMIA [a], *Miguel JORGE* [a,]*, *Miguel A. GRANATO* [a],

Filipe A. ALMEIDA PAZ [b], *Hubert CHEVREAU* [a]

and Alírio E. RODRIGUES [a,]*

[a] Laboratory of Separation and Reaction Engineering, Associate Laboratory LSRE/LCM

Department of Chemical Engineering, Faculty of Engineering, University of Porto

Rua Dr. Roberto Frias, 4200-465 Porto, Portugal

[b] CICECO, Department of Chemistry, University of Aveiro

3810-193 Aveiro, Portugal

* To whom correspondence should be addressed. Phone: 351 22 5081671. Fax: 351 22 5081674.

E-mail: mjorge@fe.up.pt; arodrig@fe.up.pt

Abstract

The separation of propane/propylene mixtures is the most energy-intensive operation practiced in the petrochemical industry. Adsorptive processes are currently viewed as a promising alternative to cryogenic distillation for the separation of these mixtures. In this paper, we explore the possibility of using a new metal-organic framework material, CuBTC, in adsorptive separation processes, particularly in a simulated moving bed (SMB) context using isobutane as a potential desorbent. A gravimetric method has been used to measure the adsorption equilibrium isotherms of propylene, propane and isobutane onto a commercial CuBTC powder over a temperature range from 323 K to 423 K and pressures up to 100 kPa. These were complemented by a detailed experimental characterization of the structure of CuBTC using XRD and SEM techniques. Comparison of experimental isotherms with grand canonical Monte Carlo simulations in CuBTC showed that propane adsorption occurs preferentially in small octahedral pockets, while isobutane is excluded from these pockets due to its bulky structure. Propylene was seen to interact strongly with unsaturated metal sites, due to specific π-Cu bonds. These interactions significantly enhance the affinity of this MOF for unsaturated hydrocarbons. Furthermore, in a range of temperatures and pressures, the affinity of CuBTC for isobutane is intermediate to that of propane and propylene. Our results suggest that CuBTC-isobutane is a very promising adsorbent-desorbent pair for use in SMB processes for propane/propylene separations.

Keywords: Adsorption, Separations, Olefin/paraffin, Porous Media, Metal-organic frameworks, Molecular Simulations

1. Introduction

Propylene is one of the most important and largest commercial volume petrochemicals in the world today. Its separation from propane/propylene streams is extremely challenging due to the physico-chemical similarities between those two molecules. Adsorptive processes have recently emerged as powerful alternatives to more conventional methods like distillation, but they require a careful choice of adsorbent for that particular separation. At the same time, tremendous progress is being made in the design of new materials, of which metal-organic frameworks (MOFs) are the most prominent example. However, advances in material synthesis have not yet been translated into widespread improvements in adsorptive process development. In this paper, we attempt to move in this direction, by exploring the possibility of applying a metal-organic framework (CuBTC) for the separation of propane and propylene. Moreover, we apply a combination of experiments and molecular simulations to provide detailed insight into the adsorption mechanism in that material, paving the way for an intelligent choice of adsorbent for olefin/paraffin separations.

The conventional method for separating propane/propylene mixtures is fractional distillation. The relative volatility for this mixture is in the range of 1.09-1.15 (Laurance and Swift, 1972; Manley and Swift, 1971) depending on composition and pressure of operation. Due to this small difference in the relative volatilities, a large number of contacting stages are needed (over 100), with a high reflux ratio, which requires a large input of energy to achieve polymer-grade propylene (> 99.5 mol %) by cryogenic distillation (Eldridge, 1993). As a result, substantial and continuing efforts have been devoted to the design and development of new and improved techniques for the separation of olefin/paraffin mixtures (Bryan, 2004). Among the different separation methods examined (e.g., extractive distillation, membranes, absorption, hydrogenation, adsorption), adsorption-based separation processes appear to be the most promising short-term solutions for providing polymer-grade propylene (Ghosh et al., 1993; Kumar et al., 1992). In fact, pressure and vacuum swing adsorption processes (Ruthven et al., 1994) have shown satisfactory results regarding product recovery (87 %) and purity (99 %) (Da Silva and Rodrigues, 2001; Grande

and Rodrigues, 2005; Rege and Yang, 2002), which prompted active research into cyclic adsorption processes for propane/propylene separation, with the continuing introduction of new adsorbents and new process cycles. In a recent patent, Rodrigues et al. (2006) have claimed that a more effective separation of this mixture can be achieved by another cyclic adsorption scheme, namely the simulated moving bed (SMB) process.

To perform this separation by means of a "conventional" SMB process (Broughton and Gerhold, 1961; Ruthven and Ching, 1989; Sá Gomes et al, 2008) it is first necessary to select a high-performance adsorbent, ideally with high adsorption capacity and selectivity. Furthermore, the adsorbent must be combined with an efficient "desorbent" – a third fluid component – that should ideally exhibit an affinity for the adsorbent that is intermediate between propane and propylene. One should highlight that the adsorbent selection cannot be independent from the choice of desorbent. In the literature, a number of commercial adsorbents have already been tested to separate C_3 components using adsorptive methods, such as commercial zeolites (4A, 5A, and 13X zeolites) (Da Silva and Rodrigues, 1999; Grande and Rodrigues, 2004; Grande et al., 2002), carbon molecular sieves (Grande et al., 2003b), or adsorbents using π-complexation agents (Padin and Yang, 2000; Yang and Kikkinides, 1995). Furthermore, isobutane was shown to be a very effective desorbent for propane/propylene SMB separations using zeolites (Lamia et al., 2007, 2008). In the last decade, a new class of porous materials with properties similar to zeolites, known as metal-organic frameworks, have been developed (Ferey, 2008; Rowsell and Yaghi, 2004). MOFs are believed to have large potential as adsorbents. These materials are hybrid structures of organic and inorganic components that possess high specific pore volumes and in some cases free coordination sites. The flexibility of their synthesis process opens the possibility of pore structure design for specific applications. In the present work a copper-based MOF was selected, the so-called CuBTC ($Cu_3(BTC)_2$, BTC = benzene-1,3,5-tricarboxylate) initially developed by Chui et al. (1999), which has showed encouraging results in terms of adsorption capacity in gas separation (Wang et al.,

2002) Furthermore, it has the added advantage of being one of the few MOF materials that are already available commercially (under the trademark Basolite® C300).

The main objective of this work is thus to determine whether CuBTC-Isobutane can be an interesting adsorbent-desorbent pair, able to operate the separation of propane/propylene mixtures by an SMB process. This requires an in-depth knowledge of the extent and mechanism of adsorption of propylene (C_3H_6), propane (C_3H_8) and isobutane (iC_4H_{10}) in CuBTC. For that purpose, we adopt a strategy that involves a combination of experimental and molecular simulation studies. Such studies have the potential to shed light into some unanswered questions regarding adsorption in MOFs (Keskin et al., 2008). Most previous simulation studies of adsorption in CuBTC have been restricted to the uptake of small gases, such as H_2, Ar, N_2, O_2, CO_2, CH_4 and H_2O (Castillo et al., 2008; Garberoglio et al., 2005; Karra and Walton, 2008; Keskin et al., 2008; Krungleviciute et al., 2007; Liu et al., 2007; Vishnyakov et al., 2003; Yang and Zhong, 2006; Yang et al., 2007). The exception is a very recent paper by Chmelik et al. (2008) dealing with alkanes, but their emphasis was on diffusion mechanisms. In the great majority of the studies mentioned above, even in those involving simple adsorbates, significant discrepancies between simulated and experimental isotherms were observed. In some cases agreement was enforced by rescaling the simulated isotherms by an arbitrary value (Krungleviciute et al., 2007) or by manipulating the interaction potential parameters (Yang and Zhong, 2006; Yang et al., 2007). However, as demonstrated recently by Keskin et al. (2008), such strategies imply a loss of transferability of the potential models, and may yield predictions that are far removed from reality. They also neglect the fact that, in some cases, disagreement may be due to impurities in the sample or to inadequate experimental procedures (Liu et al., 2007).

A more consistent approach is thus to use a combination of carefully conducted experiments and simulations, spanning a wide range of temperatures, pressures and adsorbates, to understand the phenomenon of adsorption in MOFs. In this paper, we report results of: i) detailed characterization of the material using X-ray diffraction (XRD) and Scanning Electron Microscopy (SEM); ii)

measurement of pure-component adsorption isotherms of propylene, propane and isobutane over commercial CuBTC crystals at temperatures between 323 and 423 K and pressures up to 100 kPa using a gravimetric method; iii) molecular simulation of adsorption of those hydrocarbons on CuBTC materials. The paper is organized as follows. Details of the experimental and simulation methods are given in sections 2 and 3, respectively. Section 4 presents our results, including characterization of the material structure, experimental isotherms, heats of adsorption and Henry's law constants. The isotherms are modeled using a multi-site SIPS equation and are compared to Monte Carlo simulations of adsorption in the CuBTC framework. Finally, the main conclusions are summarized in section 5.

2. Experimental

2.1 Material and adsorbates

The adsorbent used in this study is the metal-organic framework CuBTC, manufactured by Sigma Aldrich (Germany) in powder form and available under the commercial name Basolite™ C 300. Some representative properties of the adsorbent are reported in **Table 1**. The key structural characteristic of Cu_3 (BTC) $_2$ is a copper dimer with a Cu-Cu distance of 2.63 Å. These copper dimers are coordinated to the oxygen atoms of the benzene-1,3,5-tricarboxylate linkers in a paddlewheel arrangement (Chui et al., 1999). As shown in **Figure 1**, the pore structure consists of two types of cages: large main cavities, connected to each other by nearly square windows of ca. 9 Å edge, and small octahedral-shaped pockets. There are 8 pockets per unit cell, accessible from the main cavities through small triangular windows whose inscribed circle is approximately 4.6 Å in diameter. Due to the presence of copper, CuBTC provides a heterogeneous environment for polar molecules. The propane, propylene and isobutane used in this work were research-grade pure components, provided by Air Liquide (France). The purity of sorbate gases was N35 for propane (> 99.95 %), N24 for propylene (> 99.4 %) and N35 for isobutane (> 99.95 %).

Figure 1

Table 1

2.2 Experimental procedure

SEM analysis was carried out at Centro de Materiais da Universidade do Porto, Portugal, using a high-resolution JSM-6301F scanning electron microscope with a NORAN-Voyager electron diffraction spectrometer.

Conventional powder X-ray diffraction data for the bulk crystalline CuBTC were collected at ambient temperature on an X'Pert MPD Philips diffractometer (Cu $K_{\alpha 1,2}$ X-radiation, $\lambda_1 = 1.540598$ Å and $\lambda_2 = 1.544426$ Å), equipped with an X'Celerator detector and a flat-plate sample holder in a Bragg-Brentano para-focusing optics configuration (40 kV, 50 mA). Intensity data were collected by the step-counting method (step 0.01º), in continuous mode, in the ca. $3 \leq 2\theta \leq 100$º range. Variable temperature experiments were conducted on the same instrument using a high-temperature Antoon Parr HKL 16 chamber, controlled by an Antoon Parr 100 TCU unit. Consecutive data sets (range ca. $3 \leq 2\theta$º ≤ 50; step 0.03º) were collected with increasing temperature between 30 and 450 ºC, with a temperature equalization period of the sample of about 5 minutes.

The collected powder pattern of CuBTC was readily indexed using the DICVOL04 routines (implemented in the FullProf.2k software package) (Boultif and Louer, 2004) from the first 20 most intense resolved reflections (the absolute error in each reflection was fixed at 0.03 2θº). A Le Bail whole-powder-diffraction-pattern profile fitting in space group *F*m-3m was performed with FullProf.2k (Rodriguez-Carvajal, 1990; Roisnel and Rodriguez-Carvajal, 2000). Background was corrected using fixed points throughout the entire angular range determined by the linear interpolation between consecutive (and manually selected) breakpoints in the powder pattern. A typical pseudo-Voigt peak-shape function, along with two asymmetry correction parameters, was selected to generate the line shapes of the simulated diffraction peaks. The angular dependence of the full-width-at-half-maximum (FWHM) of individual reflections was also taken into account by

employing a Caglioti function correction (Caglioti et al., 1958). The overall fitting was performed in consecutive stages to avoid instability and divergence. Zero shift and all parameters related to peak shape and unit cell parameters were consecutively added as fully refineable variables upon previous full convergence of the remaining parameters to their optimal values. The corresponding Le Bail plot is provided as Electronic Supporting Material (**Figure S1**).

Adsorption measurements were performed on a magnetic suspension balance, Rubotherm (Bochum, Germany). In this method, the change of weight of a sorbent sample in the gravity field due to adsorption of molecules from a surrounding gas phase is measured. In contrast to traditional balances, the test substance is not directly connected to the balance; instead it hangs on a so-called suspension magnet. The weight gained by the substance is transmitted by magnetic suspension coupling from a closed and pressure-proof metal container to an external microbalance. The details of the balance and of its measuring principles can be found elsewhere (Dreisbach and Lösch, 2000). Advantages of the gravimetric method are the possibility of checking the activation state of a sorbent sample, its sensitivity, and its high accuracy of up to 10^{-7}.

The experimental installation used for the adsorption measurements is shown in **Figure 2**. A defined amount of adsorbent ($\cong 0.5$ g wet sample) was placed in a basket suspended by the permanent magnet through the electromagnet. The sample was submitted to a controlled temperature ramp of 2 K.min^{-1} in vacuum conditions until 423 K was reached. Activation of the sample was carried out under this temperature and 1 mbar pressure during 10 h to make sure that all water was eliminated from the sample. For the sake of rigorousness, a fresh sample was used for each adsorbate with the same activation procedure. The pure gas was then fed through tubing equipped with a valve, from the gas cylinder to the magnetic balance. Pressure and temperature in the measuring cell were measured with a Lucas Schaevitz transducer with an accuracy $\pm 5\times10^{-2}$ kPa and an Omega thermocouple with an accuracy $\pm$ 0.1 K, respectively. All measured data (mass change, pressure and temperature) were recorded by a personal computer. Adsorption equilibrium isotherms were measured at 323, 348, 373, and 423 K in the range of 0 to 100 kPa.

Figure 2

3. Simulation Details

Equilibrium adsorption isotherms were calculated using the grand canonical Monte Carlo (GCMC) technique. In this thermodynamic ensemble, the temperature (T), volume (V) and chemical potential (μ) of the system are kept fixed, while the total number of molecules (N) is allowed to fluctuate. By relating the chemical potential to the pressure (P), which is done in this work by applying the Peng-Robinson equation of state, one can compute the average adsorbed amount as a function of T and P. In order to compare the simulated isotherms to experimental data, the former need to be converted from absolute to excess adsorbed amount. For this purpose, we follow the approach of Myers and Monson (2002), and calculate the difference between absolute and excess adsorption from the second virial coefficient for Helium adsorption.

In practice, the GCMC method works by implementing several Monte Carlo trials, which are then accepted or rejected based on the rules of statistical mechanics (Frenkel and Smit, 2002). In this work we have used the standard translation and rotation trials, together with energy-biased and cavity-biased insertion and deletion trials. These special techniques significantly improve the efficiency of molecule exchange, and are essential to obtain accurate results at very high coverage. Energy bias (Snurr et al., 1993) works by preferentially inserting molecules in the regions of the solid that are energetically more favorable, while cavity bias (Mezei, 1987) works by probing regions where the sorbate molecules leave large enough cavities to accommodate a new molecule. Details of the particular implementation of these biased techniques are given by Snurr et al. (1993). All simulations were performed using the latest available version of the open-source MUSIC simulation software (Gupta et al., 2003). For each isotherm point, 5000000 equilibration steps were used, followed by 5000000 sampling steps for data collection.

The adsorbate molecules, propane, propylene and isobutane, were modeled using a united-atom description, which considers each CH_x group as a single interaction center, with effective

potential parameters. Thus, propane was composed of two $CH_3(sp^3)$ and one $CH_2(sp^3)$ centers, propylene contained one $CH_3(sp^3)$, one $CH(sp^2)$ and one $CH_2(sp^2)$ center, while isobutane was composed by one $CH(sp^3)$ and three $CH_3(sp^3)$ centers. Each site is electronically neutral and interacts with other adsorbate and framework sites by a Lennard-Jones 12-6 potential. Parameters for alkane sites were taken from the work of Dubbeldam et al. (2004), while those for alkenes were taken from Jakobtorweihen et al. (2005). These parameters provide very good agreement with experimental adsorption data of propane, propylene and isobutane in zeolites (Dubbeldam et al., 2004; Granato et al., 2007, 2008; Jakobtorweihen et al., 2005). All bond lengths were considered to be rigid, while bond angles were allowed to bend according to a harmonic angle potential, with parameters taken from the TraPPE-UA force field (Martin and Siepmann, 1998; Wick et al., 2000).

Regarding the CuBTC framework, we used a rigid all-atom representation of a single unit cell based on the crystal structure of Chui et al. (1999). This structure contains oxygen atoms bonded axially to the copper, corresponding to water ligands, but these atoms were removed in our simulations to represent a dry CuBTC sample after activation (see section 2.2). Potential parameters for the non-metallic atoms were taken from the DREIDING force field (Mayo et al., 1990) and those for the Cu atom (which were not available in DREIDING) were taken from the UFF force field (Rappé et al., 1992). These parameters were shown to yield an accurate description of hydrocarbon adsorption in IRMOF-1 and IRMOF-6 (Düren et al, 2004), which are MOFs built from the same type of organic ligand as CuBTC. Cross-species interactions were calculated from the standard Lorentz-Berthelot combining rules, and interactions were cut off at a distance of 1.3 nm. The full list of Lennard-Jones parameters is given in **Table 2**.

Table 2

4. Results and Discussion

4.1 Adsorbent characterization

Prior to the adsorption studies described in the following sub-sections, the CuBTC material was the subject of a battery of structural tests in order to unequivocally confirm both its isostructurality with the compound reported by Chui et al. (1999) and also the homogeneity of the bulk material, a pre-requisite of crucial importance for industrial applications. Scanning electron microscopy was performed to determine both morphology and size of CuBTC crystals. The SEM micrographs presented in **Figure 3**, reveal that the commercial CuBTC comprised in fact polycrystalline agglomerates of 5-10 μm, (**Figure 3.a**) interspersed with 15-20 μm octahedral-shaped crystals (**Figure 3.b**). It is worth noting that the values obtained by SEM are in good agreement with the data provided by the supplier, i.e. 16 μm.

Figure 3

A powder XRD analysis of the bulk material reveals the presence of a phase-pure and highly homogeneous crystalline sample whose structure is undoubtedly identical to that reported by Chui et al. (1999). A Le Bail whole-powder-diffraction-pattern profile fitting (see **Figure S1** in the Electronic Supporting Material) excludes the presence of either additional crystalline or amorphous materials. The stability of the hybrid crystalline framework was further investigated with increasing temperature between 30 and 450 ºC (**Figure 4**). As reported in the literature, we also registered that the dehydration of the sample does not lead to the destruction of the framework. In fact the framework remains intact until approximately 330 ºC at which temperature it collapses abruptly into an amorphous compound due, most likely, to the oxidation of the organic component. Hence, the temperatures employed for the activation of the commercial adsorbent for the studies described below do not lead either to the destruction or to the modification of the three-dimensional framework of CuBTC. Nevertheless it is also important to emphasize that this activation procedure may induce a small decrease in overall crystallinity of the material, as clearly observed by the decrease in intensity (and increase in full-width-at-half-maximum) of a handful of the reflections in the powder patterns (**Figure 4** – top).

Figure 4

4.2 Experimental pure-component adsorption isotherms

Pure-component adsorption isotherms of propane, propylene and isobutane on CuBTC at 323, 348, 373, and 423 K are shown in **Figures 5-7**. The corresponding experimental equilibrium data are reported in Electronic Supporting Material (see **Tables S1** to **S3**). The pressure is given in kPa and the absolute amount adsorbed per unit mass of adsorbent (q_i) in mol/kg.

Figure 5

Figure 6

Figure 7

In the high pressure region and at any temperature, propylene is the most adsorbed gas. This larger capacity for propylene with respect to propane has been already observed by Wagener et al. (2006, 2007). Regarding the propane adsorption isotherms it can be observed from **Figure 5** that the isotherm shape changes from type I to V with decreasing temperature. The isotherm at 373 K is clearly of type I according to the Brunauer classification (Brunauer et al., 1940)**,** while the one at 323 K is markedly different, with an S-shaped curve characteristic of type V isotherms. Regarding the adsorption isotherms of propylene presented in **Figure 6**, Langmuir-type isotherms (type I) are observed at all temperatures. Thus, one can assume a strong interaction of propylene with the surrounding framework. The nature of the strong preferential adsorption of propylene can possibly be attributed to the specific sorption interaction between the electron-rich π-bonding orbital in propylene molecules with the s-orbital of the copper atom in the CuBTC lattice. This possibility will be explored later when we compare the experimental data to molecular simulation results. In contrast, the isotherms of isobutane (**Figure 7**) are concave up to an inflection point and then reach a plateau – in other words, these isotherms can also be classified as type V (Brunauer et al., 1940). This kind of isotherm is usually observed when a molecule does not have a strong affinity for the surface until there is a significant amount bound, at which time the slope increases as the affinity for the surface increases. This may occur if the adsorbate molecule modifies the surface or begins to

bind to previously bound molecules. The plateau occurs when saturation is reached. It is also worth noting that the isobutane adsorption equilibrium isotherms measured in this work are in qualitative agreement with measurements performed at 303 K by Hartmann et al. (2008).

4.3 Isosteric heat of adsorption and Henry's law constants

Information related to the isosteric heat of adsorption and its variation with respect to the loading can provide useful information about surface characteristics and the adsorbed phase. In fact, surface characteristics can be assessed by determining the heat of adsorption released as the adsorbate interacts with the adsorbent cages at a given loading. The isosteric heat of adsorption (Q_{st}) of a single component can be calculated using the Clausius-Clapeyron relationship:

$$Q_{st} = R T^2 \left(\frac{\partial \ln P}{\partial T} \right)_{q_i} \qquad (1)$$

Cross plotting yields sets of P vs. T relations at constant q, from which values for Q_{st} can be obtained.

In **Figure 8**, the isosteric heats of adsorption of the studied adsorbates are shown as a function of loading, and the average values are reported in **Table 3**. As can be seen in **Figure 8** the isosteric heats of all adsorbates do not remain constant with increasing adsorbate loading. These significant variations can be explained by enhanced interactions between the molecules in the adsorbed phase, and highlight the energetic heterogeneity of the adsorbent surface. For instance, the heat of adsorption for propylene decreases with coverage, which reveals a strong specific interaction of this adsorbate with the CuBTC framework. On the contrary, the heat of adsorption for isobutane increases with coverage, which means that the affinity of the adsorbent for isobutane is enhanced by the presence of other isobutane molecules. The average values of the isosteric heat of adsorption for propane and isobutane compare well with previous reports (Hartmann et al., 2008; Wagener et al., 2006, 2007), while our result for propylene is somewhat higher than the value reported by Wagener et al. (2006, 2007).

Figure 8

Table 3

It is also useful to evaluate the Henry's law constant (H) in order to understand the interaction between the adsorbate molecules and the sorbent surface. Extraction of H from the pure-component adsorption isotherms is simply achieved by plotting q/P versus q and extrapolating thereafter the intercept by fitting all of the q/P data by a cubic polynomial in q:

$$H = \lim_{P \to 0} \frac{\partial q}{\partial P} = \lim_{q \to 0} \frac{\partial q}{\partial P} \quad \text{and} \quad \frac{q}{P} = \alpha_0 + \alpha_1 q + \alpha_2 q^2 + \alpha_3 q^3 \qquad (2)$$

The extracted values are reported in **Table 3** for propane, propylene and isobutane at different temperatures. As expected, the Henry's law constants of all adsorbates decrease with increasing temperature. One should also notice that the value of H for isobutane is intermediate to the ones of propane and propylene.

4.4 Dual site Sips model

A number of equilibrium isotherm models can be used to fit experimental equilibrium data (Do, 1998). In this work the Dual Site Sips (DSS) model was chosen to describe all the experimental adsorption isotherms. Being a thermodynamically consistent model, this equation is more efficient than the multisite Langmuir model for fitting most of the adsorption data. On the other hand, compared with other thermodynamic models, it gives with great simplicity a quantitative description of the observed equilibria, and can be used easily in non-isothermal simulated moving bed simulations. The DSS equation was applied in the following form:

$$q_i = q_{m,i,A} \frac{\left(b_{i,A} P\right)^{1/\eta_{i,A}}}{1 + \left(b_{i,A} P\right)^{1/\eta_{i,A}}} + q_{m,i,B} \frac{\left(b_{i,B} P\right)^{1/\eta_{i,B}}}{1 + \left(b_{i,B} P\right)^{1/\eta_{i,B}}} \qquad (3)$$

$$\text{and} \quad b_i = b_{i,0} \, exp\left(\frac{Q_{st}}{RT}\left(1 - \frac{T}{T_0}\right)\right) \quad \text{with} \quad T_0 = 323 \text{ K} \qquad (4)$$

where q_i is the absolute adsorbed amount of the single component i, $q_{m,i}$ is the maximum loading capacity of the sorbent, b_i is the affinity parameter of the pure component i for the solid sorbent, and Q_{st} is the isosteric heat of adsorption at zero loading. The coefficient η_i represents the solid heterogeneity parameter and is assumed here to be independent of temperature. It is worth pointing out that the DSS model reduces to the multisite Langmuir equation for a heterogeneity parameter $\eta_i = 1$. The DSS model has been applied successfully to describe different adsorption systems, in particular the adsorption of different pure hydrocarbons on CuBTC (Chmelik et al., 2008).

There are several ways to evaluate the precision of a fit to a set of experimental data. A commonly used parameter for adsorption isotherms is the average relative error (ARE), defined as follows:

$$ARE = \frac{100}{N} \times \sum_{k=1}^{N} \left| \frac{q_{exp} - q_{cal}}{q_{exp}} \right|_k \qquad (5)$$

where N is the number of data points, q_{exp} and q_{cal} are the experimental and the calculated amount adsorbed, respectively.

The fits obtained from the DSS model are represented with solid lines in **Figures 5-7**. The optimal fitting parameters were obtained through an optimization routine in the MATLAB software (7.3) by minimizing the sum square of residuals between the experimental data and the DSS equation. The values of these model parameters are summarized in **Table 4**. Interestingly, the adsorption heats determined using the DSS model are in good agreement with the isosteric heats calculated in this work using Eq. (1). The experimental results of the three gases are well correlated with this model. In **Table 5** the average relative error between experimental data and correlated results is listed. The ARE values are in the range of experimental error and demonstrate indeed a good agreement between the experimental isotherms and the results of the DSS model.

Table 4

Table 5

4.5 Molecular simulation of adsorption

In **Figure 9a**, we compare the experimental adsorption isotherm for isobutane at 373 K with molecular simulation on the full CuBTC structure. It is clear that the simulations, shown as the full line, significantly overestimate the experimental data. There is a possible explanation for this, based on the structure of the CuBTC framework. As described in section 2.1, it is composed of two types of pores: large cavities and small pockets. Although an isobutane molecule may fit inside an octahedral pocket, it cannot access it through the small triangular windows due to its large collision diameter, which is a direct consequence of the branched structure of isobutane. Thus, in a real adsorption experiment, the pockets are effectively excluded from isobutane adsorption. In a GCMC simulation, on the other hand, molecule insertions are attempted in the whole volume with equal probability. Thus, an isobutane molecule can "appear" in one of the pockets, and take advantage of the energetically favorable environment, without ever having to diffuse inside it. This can be seen in the snapshot of **Figure 10a**, where adsorbed isobutane molecules appear in the pockets at very low pressure. The result is an overestimation of the amount adsorbed in the simulations at all pressures.

Figure 9

Figure 10

To circumvent this problem, we have repeated our GCMC simulations in CuBTC, but now preventing adsorption in the pockets. In practice, this was achieved by placing a repulsive sphere of 3 Å in diameter at the center of each pocket. This procedure effectively excludes isobutane adsorption in the pockets, as is clear from the snapshot of **Figure 10b**. The result of such a simulation for isobutane at 373 K is shown in **Figure 9a** as the dashed line. As we can see, the agreement between simulation and experiment is remarkable, confirming our hypothesis. In **Figure 9b**, we present comparisons between experimental data and simulations using the blocked framework for isobutane at all temperatures. Good agreement was obtained in all cases.

Comparisons between simulation and experiment were also carried out for pure propane adsorption. These are shown in **Figure 11a** at 348 K. Once more, the simulation results considering the entire pore space of the CuBTC structure (full line) overestimate the experimental data, but now the difference is much more pronounced at high pressure than at low pressure. From the snapshots in **Figure 12**, one can see that propane adsorption occurs preferentially in the octahedral pockets at low pressure (**Figure 12a**) and in both cages at high pressure (**Figure 12b**). To test whether the discrepancy between simulation and experiment is due to inaccessible pockets, we performed simulations in the blocked CuBTC structure using the same procedure as for isobutane. The simulation results (dashed line in **Figure 11a**) now underestimate adsorption at low pressure, but seem to converge to the correct limiting coverage at high pressure. The fact that the experimental data at low pressure is much closer to the simulation in the full structure suggests that propane is indeed adsorbing in the pockets at low pressure. This is a reasonable expectation, since propane is a linear hydrocarbon with a radial cross-section that is smaller than the diameter of the small windows (about 4.6 Å). Indeed, the pattern is the same at all temperatures (see **Figure 11b**) – reasonable agreement between simulation and experiment at low pressure and consistent overestimation by about 20% at high pressure.

Figure 11

Figure 12

Having established that propane does adsorb in the small pockets, we are left with explaining the differences at high pressure. Since the adsorption experiments were performed by incremental increases in pressure (i.e., once the adsorbed amount equilibrates for a given pressure value, the pressure is increased stepwise to the next point, and so on), it is reasonable to expect that the propane molecules that were adsorbed in the pockets at low pressure remain there at high pressure. Therefore, it seems that the agreement between experiments and simulations in the blocked CuBTC structure in the high-pressure limit are fortuitous. A more likely explanation is the difficulty in reaching equilibrium in the propane adsorption experiments at high coverage. A similar

phenomenon was previously observed in zeolite 4A (Grande et al., 2003a), which also possesses a structure comprising both small and large cages connected by small windows. We are currently performing tests in the laboratory to check whether this is indeed the case.

The case of propylene adsorption presents a completely different scenario. As we can see from **Figure 13a**, simulations in both the full CuBTC and the blocked CuBTC structures dramatically underestimate the amount adsorbed. Such a discrepancy clearly points to an inadequacy in the force field describing propylene-CuBTC interactions. The force field describes only van der Waals interactions between the adsorbate and adsorbent sites, which are particularly weak when they involve copper atoms (see low value of ε for this atom in **Table 3**). After the removal of Cu-coordinated water molecules during the activation procedure, each copper atom is penta-coordinated, and thus possesses an unsaturated site. The existence of a specific interaction between the π orbitals of the sp^2 sites of propylene and the unsaturated metal sites is very likely, and is unaccounted for in standard force fields.

Figure 13

As a simplified approach for describing these specific interactions, we have empirically changed the value of ε for Cu interacting with the $CH_2(sp^2)$ and $CH(sp^2)$ sites of propylene (maintaining the standard combination rules). The value of this parameter was adjusted so that the result of a simulation of pure propylene at 323 K and 10 kPa matched the experimental value (see **Figure 13a**). This point was chosen because it lies on the upward curve of the isotherm at the lowest temperature, thus providing a stringent test for the potential. The resulting value of ε/k_B was 875 K, yielding a total interaction energy between Cu and the two sp^2 sites of the order of 16 kJ/mol, which is within the expected range for π-metal interactions (Humphrey and Keller II, 1997). This strong specific interaction enhances the affinity of the framework for propylene, strongly increasing its uptake (compare the two snapshots of **Figure 14**).

Figure 14

Using this modified interaction potential, we are able to obtain good agreement between simulation and experiment at all temperatures (**Figure 13b**). This agreement is even more remarkable given the rather crude nature of our approach for describing π-Cu interactions. In fact, it is unlikely that this type of interaction is fundamentally described by a Lennard-Jones 12-6 functional form, and thus a more chemically consistent approach is desirable. This could be based on the inclusion of partial charges in the framework and adsorbates (Castillo et al., 2008; Karra and Walton, 2008) or on the addition of a specific term for π-metal bonds (Blas et al., 1998). Nevertheless, the good description of experimental data strongly suggests that the high uptake of propylene is due to strong specific π-Cu bonds. This interpretation agrees with visual inspection of the powder samples after adsorption of the different hydrocarbons – in the case of propane and isobutane the powder showed a deep blue color, while samples after propylene adsorption showed a distinctive turquoise color, similar to that of the hydrated sample. Changes of color of copper complexes with the degree of metal coordination are well known (Miessler and Tarr, 2004), and thus these observations corroborate our conclusion that propylene occupies the coordination sites left vacant after the removal of water molecules.

4.6 Suitability of CuBTC / Isobutane as adsorbent / desorbent couple

In order to assess the potential of CuBTC for use in olefin/paraffin separations, we performed a comparison of adsorption equilibrium isotherms of propane and propylene on this material with the ones obtained from adsorbents commonly used for that type of separation (Grande et al., 2003b; Lamia et al., 2007), which is shown in **Figure 15**. As seen in this figure the adsorption capacities of CuBTC for both species are three to four times higher than those of 13X zeolite and carbon molecular sieves.

Figure 15

Figure 16a shows the 373 K isotherms for propane (C_3H_8), propylene (C_3H_6) and isobutane (iC_4H_{10}) in the pressure range of 0 to 100 kPa. At low pressures the isobutane isotherm exhibits the

greatest slope and the highest adsorption capacity. The C_3H_8 and C_3H_6 isotherms have a more gradual slope at low pressure but continue to show increases in the amount adsorbed at pressures far greater than the value at which the iC_4H_{10} isotherm levels off. On the other hand, in this pressure range ($P \geq 50$ kPa), it can be observed that the isobutane isotherm is markedly intermediate to the two C_3 component isotherms. Furthermore, regarding the loading capacities reported in **Table 4**, it can be observed that isobutane is *de facto* intermediate to propylene and propane. This suggests that at 373 K isobutane can be a potential desorbent in the context of a propane-propylene separation by SMB. Although this information is interesting, such a conclusion cannot be drawn only from single-component adsorption isotherms.

Figure 16

Another way to point out the intermediate selectivity of isobutane with respect to C_3 components is to plot the Henry's law constants calculated previously for different temperatures (see section 4.3) as a function of inverse temperature (**Figure 16b**). Although the calculated Henry's constants are extrapolations based on the isotherms used, this figure nevertheless allows us to identify the following selectivity sequence: propylene > isobutane > propane. It is worth pointing out that propylene has indeed the highest Henry's law constant among the adsorbates studied which confirms again the strong affinity of CuBTC for propylene. Considering this observation, isobutane could be used as a possible desorbent in combination with CuBTC in a simulated moving bed process.

5. Conclusions

In this paper, we report new adsorption isotherms, isosteric heats of adsorption and Henry's law constants for propane, propylene and isobutane over CuBTC crystals, measured by a gravimetric method. These measurements were compared to molecular simulation results and supported by a detailed structural characterization analysis, enabling us to elucidate the mechanisms of adsorption of those hydrocarbons in the MOF framework. Our results show that at low pressure

propane adsorbs preferentially in the small octahedral pockets available in the framework, while at high pressure, adsorption occurs also in the large cages. Differences between experimental and simulated isotherms at high pressure are possibly due to difficulties in reaching true equilibrium in the experimental measurements, caused by the slow diffusion of propane. Further tests are required to confirm this hypothesis. Comparison between simulation and experiment for isobutane shows that this molecule is excluded from the pockets, which explains the s-shaped nature of the adsorption isotherm. This interpretation agrees with our analysis of the heats of adsorption for isobutane.

Regarding propylene, a very interesting effect was observed – our results point to the existence of strong specific interactions between the π orbitals of this adsorbate and unsaturated Cu sites, left vacant after the removal of weakly-coordinated water molecules during activation. Indeed, by accounting for these strong interactions in a very approximate way, we are able to obtain good agreement between simulation and experiment in the entire range of temperatures and pressures studied. This conclusion is supported by the observed decrease in the isosteric heat of adsorption of propylene with increasing coverage, and by visual observation of the striking color change of the powder sample upon propylene adsorption. Nevertheless, further work is necessary to include a more chemically reasonable description of π-metal interactions that is transferrable to other adsorbates and MOF frameworks.

Finally, we have shown that CuBTC possesses a significantly higher adsorption capacity for propane and propylene relative to standard commercial adsorbents. Comparison of the adsorption equilibrium isotherms and Henry's law constants shows that, in well-defined ranges of pressure and temperature, the affinity of CuBTC for isobutane is intermediate to that of propane and propylene. These observations suggest that CuBTC-Isobutane can be a pertinent adsorbent/desorbent couple in a classical SMB mode of operation for the separation of propane/propylene mixtures. Our study paves the way for the future integration of novel MOF materials in industrial adsorptive separation processes.

Electronic Supplementary Material: Le Bail whole-powder-diffraction-pattern profile fitting to the XRD pattern of CuBTC, and experimental data for adsorption of propane, propylene and isobutane.

Acknowledgements

FAAP acknowledges *Fundação para a Ciência e a Tecnologia* (FCT, Portugal) for the financial support towards the upgrade of the powder X-ray diffractometer (University of Aveiro).

References

Blas, F.J., Vega, L.F., Gubbins, K.E., 1998. Modeling new adsorbents for ethylene/ethane separations by adsorption via pi-complexation. Fluid Phase Equil. 150-151, 117.

Boultif, A., Louer, D. J., 2004. Powder pattern indexing with the dichotomy method. Appl. Crystallogr. 37, 724.

Broughton, D.B., Gerhold, C.G., 1961. Continuous Sorption Process Employing Fixed bed of Sorbent and Moving Inlets and Outlets. U.S. Patent 2,985,589.

Brunauer, S., Deming, L., Deming, W.E., Teller, E., 1940. On a theory of the van der Waals adsorption of gases. J. Am. Chem. Soc. 62, 1723.

Bryan, P.F., 2004. Removal of propylene from fuel-grade propane. Sep. Pur. Rev. 33, 157.

Caglioti, G., Paoletti, A., Ricci, F. P., 1958. Choice of collimators for a crystal spectrometer for neutron diffraction. Nucl. Instr. 3, 223.

Castillo, J.M., Vlugt, T.J.H., Calero, S., 2008. Understanding water adsorption in Cu-BTC metal-organic frameworks. J. Phys. Chem. C 112, 15934.

Chmelik, C., Kärger, J., Wiebcke, M., Caro, J., Van Baten, J.M., Krishna R., 2008. Adsorption and diffusion of alkanes in CuBTC crystals investigated using infra-red microscopy and molecular simulations. Micropor. Mesopor. Mater, in press: doi:10.1016/j.micromeso.2008.06.003.

Chui, S.S.Y., Lo, S.M.F., Charmant, J.P.H., Orpen, A.G., Williams, I.D., 1999. A chemically functionalizable nanoporous material [Cu-3(TMA)(2)(H2O)(3)](n). Science 283, 1148.

Da Silva, F.A., Rodrigues, A.E., 1999. Adsorption equilibria and kinetics for propylene and propane over 13X and 4A zeolite pellets. Ind. Eng. Chem. Res. 38, 2051.

Da Silva, F.A., Rodrigues, A.E., 2001. Propylene/propane separation by vacuum swing adsorption using 13X zeolite. AIChE J. 47, 341.

Do, D.D., 1998. Adsorption analysis: Equilibria and kinetics. Imperial College Press, London, U.K.

Dreisbach, F., Lösch, H.W., 2000. Magnetic suspension balance for simultaneous measurement of a sample and the density of the measuring fluid. J. Therm. Anal. Calorim. 62, 515.

Dubbeldam, D., Calero, S., Vlugt, T.J.H., Krishna, R., Maesen, T.L.M., Smit, B., 2004. United atom force field for alkanes in nanoporous materials. J. Phys. Chem. B 108, 12301.

Düren, T., Sarkisov, L., Yaghi, O.M., Snurr, R.Q., 2004. Design of new materials for methane storage. Langmuir 20, 2683.

Eldridge, R.B., 1993. Olefin paraffin separation technology – a review. Ind. Eng. Chem. Res. 32, 2208.

Ferey, G., 2008. Hybrid porous solids: past, present, future. Chem. Soc. Rev. 37, 191.

Frenkel, D., Smit, B., 2002. Understanding molecular simulation. Academic Press, San Diego, USA.

Garberoglio, G., Skoulidas, A.I., Johnson, J.K., 2005. Adsorption of gases in metal organic materials: Comparison of simulations and experiments. J. Phys. Chem. B 109, 13094.

Ghosh, T.K., Lin, H.D., Hines, A.L., 1993. Hybrid adsorption distillation process for separating propane and propylene. Ind. Eng. Chem. Res. 32, 2390.

Granato, M.A., Lamia, N., Vlugt, T.J.H., Rodrigues, A.E., 2008. Adsorption equilibrium of isobutane and 1-butene in zeolite 13X by molecular simulation. Ind. Eng. Chem. Res. 47, 6166.

Granato, M.A., Vlugt, T.J.H., Rodrigues, A.E., 2007. Molecular simulation of propane-propylene binary adsorption equilibrium in zeolite 13X. Ind. Eng. Chem. Res. 46, 7239.

Grande, C.A., Rodrigues, A.E., 2004. Adsorption kinetics of propane and propylene in zeolite 4A. Chem. Eng. Res. Des. 82, 1604.

Grande, C.A., Rodrigues, A.E., 2005. Propane/propylene separation by pressure swing adsorption using zeolite 4A. Ind. Eng. Chem. Res. 44, 8815.

Grande, C.A., Gigola, C., Rodrigues, A.E., 2002. Adsorption of propane and propylene in pellets and crystals of 5A zeolite. Ind. Eng. Chem. Res. 41, 85.

Grande, C.A., Gigola, C., Rodrigues, A.E., 2003a. Propane-propylene binary adsorption on zeolite 4A. Adsorption, 9, 321.

Grande, C.A., Silva, V.M.T.M., Gigola, C., Rodrigues, A.E., 2003b. Adsorption of propane and propylene onto carbon molecular sieve. Carbon 41, 2533.

Gupta, A., Chempath, S., Sanborn, M.J., Clark, L.A., Snurr, R.Q., 2003. Object-oriented programming paradigms for molecular modeling. Mol. Simul. 29, 29.

Hartmann, M., Kunz, S., Himsl, D., Tangermann, O., 2008. Adsorptive separation of isobutene and isobutane on Cu-3(BTC)(2). Langmuir 24, 8634.

Humphrey, J.L., Keller II, G.E., 1997. Separation process technology. McGraw-Hill, New York.

Jakobtorweihen, S., Hansen, N., Keil, F., 2005. Molecular simulation of alkene adsorption in zeolites. Mol. Phys. 103, 471.

Karra, J.R., Walton, K.S., 2008. Effect of open metal sites on adsorption of polar and nonpolar molecules in metal-organic framework Cu-BTC. Langmuir 24, 8620.

Keskin, S., Liu, J., Rankin, R.B., Johnson, J.K., Sholl, D.S., 2008. Progress, opportunities, and challenges for applying atomically detailed modeling to molecular adsorption and transport in metal-organic framework materials. Ind. Eng. Chem. Res., in press; doi: 10.1021/ie800666s.

Krungleviciute, V., Lask, K., Heroux, L., Migone, A.D., Lee, J.-Y., Li, J., Skoulidas, A., 2007. Argon adsorption on Cu-3(Benzene-1,3,5-tricarboxylate)(2)(H2O)(3) metal-organic framework. Langmuir, 23, 3106.

Kumar, R., Golden, T.C., White, T.R., Rokicki, A., 1992. Novel adsorption distillation hybrid scheme for propane propylene separation. Sep. Tech. 15, 2157.

Lamia, N., Wolff, L., Leflaive, P., Leinekugel-le-Cocq, D., Sá Gomes, P., Grande, C.A., Rodrigues, A.E., 2008. Equilibrium and fixed bed adsorption of 1-butene, propylene and propane over 13X zeolite pellets. Sep. Sci. and Tech. 43, 1124.

Lamia, N., Wolff, L., Leflaive, P., Sá Gomes, P., Grande, C.A., Rodrigues, A.E., 2007. Propane/propylene separation by simulated moving bed I. Adsorption of propane, propylene and isobutane in pellets of 13X zeolite. Sep. Sci. and Tech. 42, 2539.

Laurance, D. R., Swift, G.W., 1972. Relative volatility of propane-propene system from 100-160-degrees F. J. Chem. Eng. Data 17, 333.

Liu, J., Culp, J.T., Natesakhawat, S., Bockrath, B.C., Zande, B., Sankar, S.G., Garberoglio, G., Johnson, J.K., 2007. Experimental and theoretical studies of gas adsorption in Cu-3(BTC)(2): An effective activation procedure. J. Phys. Chem. C 111, 9305.

Manley, D. B., Swift, G. W., 1971. Relative volatility of propane-propene system by integration of general coexistence equation. J. Chem. Eng. Data 16, 301.

Martin, M.G., Siepmann, J.I., 1998. Transferable potentials for phase equilibria. 1. United-atom description of n-alkanes. J. Phys. Chem. B 102, 2569.

Mayo, S.L., Olafson, B.D., Goddard III, W.A., 1990. DREIDING – A generic force-field for molecular simulations. J. Phys. Chem 94, 8897.

Mezei, M., 1987. Grand-canonical ensemble Monte Carlo study of dense liquid Lennard-Jones, soft spheres and water. Mol. Phys. 61, 565.

Miessler, G. L., Tarr, D. A., 2004. Inorganic chemistry. Third Ed., Pearson Prentice Hall, Upper Saddle River, NJ, USA.

Myers, A.L., Monson, P.A., 2002. Adsorption in porous materials at high pressure: Theory and experiment. Langmuir 18, 10261.

Padin, J., Yang, R.T., 2000. New sorbents for olefin/paraffin separations by adsorption via pi-complexation: synthesis and effects of substrates. Chem. Eng. Sci. 55, 2607.

Rappé, A.K., Casewit, C.J., Colwell, K.S., Goddard III, W.A., Skiff, W.M., 1992. UFF, a full periodic-table force-field for molecular mechanics and molecular-dynamics simulations. J. Am. Chem. Soc. 114, 10024.

Rege, S.U., Yang, R.T., 2002. Propane/propylene separation by pressure swing adsorption: sorbent comparison and multiplicity of cyclic steady states. Chem. Eng. Sci. 57, 1139.

Rodrigues, A.E., Lamia, N., Grande, C.A., Wolff, L., Leflaive, P., Leinekugel-le-Cocq, D., 2006. Procédé de Séparation du Propylène en Mélange avec du Propane par Adsorption en Lit Mobile Simulé en Phase Gaz ou Liquide utilisant une Zéolithe de type Faujasite 13X comme Solide Adsorbant. FR. Patent 2.903.981; Int. Patent WO.2008.012410.

Rodriguez-Carvajal, J., 1990. FULLPROF - A program for Rietveld refinement and pattern matching analysis, Abstract of the Satellite Meeting on Powder Diffraction of the XV Congress of the IUCR, Toulouse, France 127.

Roisnel, T., Rodriguez-Carvajal, J., 2000. WinPLOTR - A Windows tool for powder diffraction pattern analysis. Materials Science Forum, Proceedings of the Seventh European Powder Diffraction Conference (EPDIC 7), Ed. R. Delhez and E.J. Mittenmeijer 118.

Rowsell, J.L.C., Yaghi, O.M., 2004. Metal-organic frameworks: a new class of porous materials. Micropor. Mesopor. Mater. 73, 3.

Ruthven, D.M., Ching, C.B., 1989. Countercurrent and simulated countercurrent adsorption separation processes. Chem. Eng. Sci. 44, 1011.

Ruthven, D.M., Farooq, S., Knaebel, K.S., 1994. Pressure Swing Adsorption. VCH Publishers, New York, USA.

Sá Gomes, P., Lamia, N., Rodrigues, A.E., 2008. Design of a gas phase simulated moving bed for propane/propylene separation. Chem. Eng. Sci., in press; doi:10.1016/j.ces.2008.11.022.

Snurr, R.Q., Bell, A.T., Theodorou, D.N., 1993. Prediction of adsorption of aromatic-hydrocarbons in silicalite from grand-canonical Monte Carlo simulations with biased insertions. J. Phys. Chem. 97, 13742.

Vishnyakov, A., Ravikovitch, P.I., Neimark, A.V., Bülow, M., Wang, Q.M., 2003. Nanopore structure and sorption properties of Cu-BTC metal-organic framework. Nano Lett. 3, 713.

Wagener, A., Rudolphi, F., Schindler, M., Ernst, S., 2006. Separation of propane/propene mixtures by adsorption on metal organic coordination polymers. Chem. Ing. Tech. 78, 1328.

Wagener, A., Schindler, M., Rudolphi, F., Ernst, S., 2007. Metal-organic coordination polymers for the adsorptive separation of propane/propylene compounds. Chem. Ing. Tech. 79, 851.

Wang, Q., Shen, D., Bülow, M., Lau, M., Deng, S., Fitch, F.R., Lemcoff, N.O., Semanscin J., 2002. Metallo-organic molecular sieve for gas separation and purification. Micropor. Mesopor. Mater. 55, 217.

Wick, C.D., Martin, M.G., Siepmann, J.I., 2000. Transferable potentials for phase equilibria. 4. United-atom description of linear and branched alkenes and alkylbenzenes. J. Phys. Chem. B 104, 8008.

Yang, Q., Zhong, C., 2006. Molecular simulation of carbon dioxide/methane/hydrogen mixture adsorption in metal-organic frameworks. J. Phys. Chem. B, 110, 17776.

Yang, Q., Xue, C., Zhong, C., Chen, J.-F., 2007. Molecular simulation of separation of CO2 from flue gases in Cu-BTC metal-organic framework. AIChE J. 53, 2832.

Yang, R.T., Kikkinides, E.S., 1995. New sorbents for olefin paraffin separations by adsorption via pi-complexation. AIChE. J. 41, 509.

Table Captions

Table 1. Physical properties of the adsorbent studied

Table 2. Lennard-Jones potential parameters for hydrocarbons and CuBTC atoms

Table 3. Henry's law constants at different temperatures and isosteric heat of adsorption

Table 4. Adsorption equilibrium parameters of the Dual Site Sips model on CuBTC crystal

Table 5. Average relative error (ARE) between experimental data and correlated results (%)

Figure captions

Figure 1. Framework structure of CuBTC viewed along two directions. (a) [100]; (b) [111]. (Color key: yellow = copper, red = oxygen, green = carbon, white = hydrogen)

Figure 2. Schematic diagram of the experimental setup used for the adsorption equilibrium measurements.

Figure 3. SEM pictures of CuBTC (Basolite ® C300): (a) polycrystalline; (b) single crystal.

Figure 4. 3D (*top*) and 2D (*bottom*) representations of the variation of the powder X-ray diffraction pattern of CuBTC (Basolite™ C 300) with increasing temperature under air atmosphere. After approximately 330ºC the destruction of the framework is notorious, with the complete disappearance of the first and most intense reflections characteristic of CuBTC, forming an amorphous compound.

Figure 5. Adsorption equilibrium isotherms of propane on CuBTC at different temperatures. Solid lines represent the Dual Site Sips model fits.

Figure 6. Adsorption equilibrium isotherms of propylene on CuBTC at different temperatures. Solid lines represent the Dual Site Sips model fits.

Figure 7. Adsorption equilibrium isotherms of isobutane on CuBTC at different temperatures. Solid lines represent the Dual Site Sips model fits.

Figure 8. Isosteric heat of adsorption as a function of the amount adsorbed for each adsorbate a) propane; b) propylene; c) isobutane.

Figure 9. a) Comparison of experimental isobutane adsorption (circles) at 373 K with molecular simulations using the full CuBTC structure (full line) and using the CuBTC structure with blocked tetrahedral pockets (dashed line); b) Comparison of experimental isobutane adsorption (symbols) with simulations using the blocked CuBTC structure (lines) at all temperatures.

Figure 10. Snapshots of adsorption simulations for isobutane at 373 K and 3.5 kPa using: a) the full CuBTC structure; b) the blocked CuBTC structure. Color coding for the framework atoms is the same as in Figure 1 and isobutane sites are shown as dark blue spheres.

Figure 11. a) Comparison of experimental propane adsorption (circles) at 348 K with molecular simulations using the full CuBTC structure (full line) and using the CuBTC structure with blocked tetrahedral pockets (dashed line); b) Comparison of experimental propane adsorption (symbols) with simulations using the full CuBTC structure (lines) at all temperatures.

Figure 12. Snapshots of adsorption simulations for propane in the full CuBTC structure at 348 K and: a) 5 kPa; b) 100 kPa. Color coding for the framework atoms is the same as in Figure 1 and propane sites are shown as light blue spheres.

Figure 13. a) Comparison of experimental propylene adsorption (circles) at 323 K with molecular simulations using the full CuBTC structure (full line), using the CuBTC structure with blocked tetrahedral pockets (dashed line), and using the full structure with the modified potential to account for π-Cu interactions (dashed-dotted line); b) Comparison of experimental propylene adsorption (symbols) with simulations using the full CuBTC structure with the π-Cu potential (lines) at all temperatures.

Figure 14. Snapshots of adsorption simulations for propylene at 373 K and 5 kPa in the full CuBTC structure using: a) the standard potential; b) the modified potential accounting for π-Cu interactions. Color coding for the framework atoms is the same as in Figure 1 and propylene sites are shown as purple spheres.

Figure 15. Comparison of experimental adsorption isotherm data of propane (top) and propylene (bottom) on different adsorbents (zeolite 13X (Lamia et al., 2007), carbon molecular sieve 4A (Grande et al., 2003b) and CuBTC) at 373 K.

Figure 16. a) Single adsorption isotherms of propane, propylene and isobutane on CuBTC at 373 K (solid lines are the DSS model fits) ; b) Arrhenius plot of Henry constant values obtained from the experimental adsorption isotherms.

Table 1. Physical properties of the adsorbent studied

Property	CuBTC
Commercial name	Basolite ® C300
Supplier	Sigma-Aldrich
Activation conditions	423 K under vacuum (10 h)
Molecular weight	605 g/mol
Particle size	16 μm
Bulk density	350 kg/m^3
BET surface area	1500-2100 m^2/g

Table 2. Lennard-Jones potential parameters for hydrocarbons and CuBTC atoms

Site	σ (nm)	ε/k_B (K)
CH_3 (sp^3)	0.3760	108.00
CH_s (sp^3)	0.3960	56.00
CH (sp^3)	0.4670	17.00
CH_2 (sp^2)	0.3675	85.00
CH (sp^2)	0.3730	47.00
Cu	0.3114	2.514
O	0.3033	48.16
C	0.3476	47.86
H	0.2846	7.650

Table 3. Henry's law constants at different temperatures and isosteric heat of adsorption

	$H_{323\ K}$ ($mol.kg^{-1}.kPa^{-1}$)	$H_{348\ K}$ ($mol.kg^{-1}.kPa^{-1}$)	$H_{373\ K}$ ($mol.kg^{-1}.kPa^{-1}$)	$H_{423\ K}$ ($mol.kg^{-1}.kPa^{-1}$)	$Q_{st}^{this\ work}$ (kJ/mol)	$Q_{st}^{literature}$ (kJ/mol)
Propane	0.458	0.2145	0.1008	0.0152	28.5	30.0 [a]
Propylene	10.589	1.6756	0.4526	0.0738	41.8	33.0 [a]
Isobutane	2.324	0.6309	0.2376	0.0513	38.0	42.0 [b]

[a] – Taken from Wagener et al., 2007.

[b] – Taken from Hartmann et al., 2008.

Table 4. Adsorption equilibrium parameters of the Dual Site Sips model on CuBTC crystal

Adsorbate	$q_{m,i,A}$ (mol/kg)	$b_{i,A,0}$ (kPa^{-1})	$Q_{st,i,A}$ (kJ/mol)	$\eta_{i,A}$ (-)	$q_{m,i,B}$ (mol/kg)	$b_{i,B,0}$ (kPa^{-1})	$Q_{st,i,B}$ (kJ/mol)	$\eta_{i,B}$ (-)
Propane	6.21	0.07	28.7	0.82	1.14	0.16	34.1	0.32
Propylene	7.09	0.42	41.9	1.00	1.22	0.06	47.0	0.80
Isobutane	5.12	0.82	37.9	0.55	1.10	0.06	40.8	1.00

Table 5. Average relative error (ARE) between experimental data and correlated results (%)

Temperature (K)	Propane	Propylene	Isobutane
323	0.409	5.103	4.505
348	2.777	8.235	6.473
373	2.842	2.016	2.608
423	5.516	2.371	5.321

Figure1

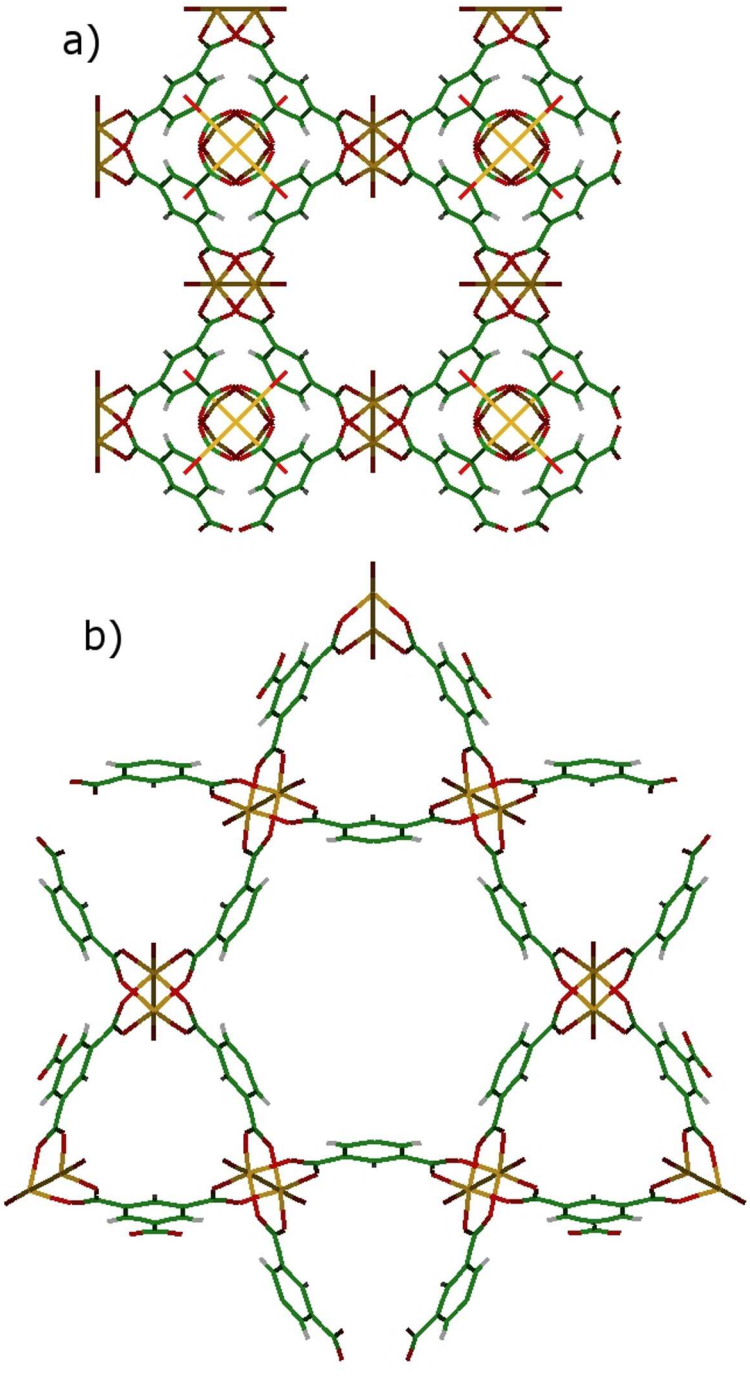

Figure2

Click here to download high resolution image

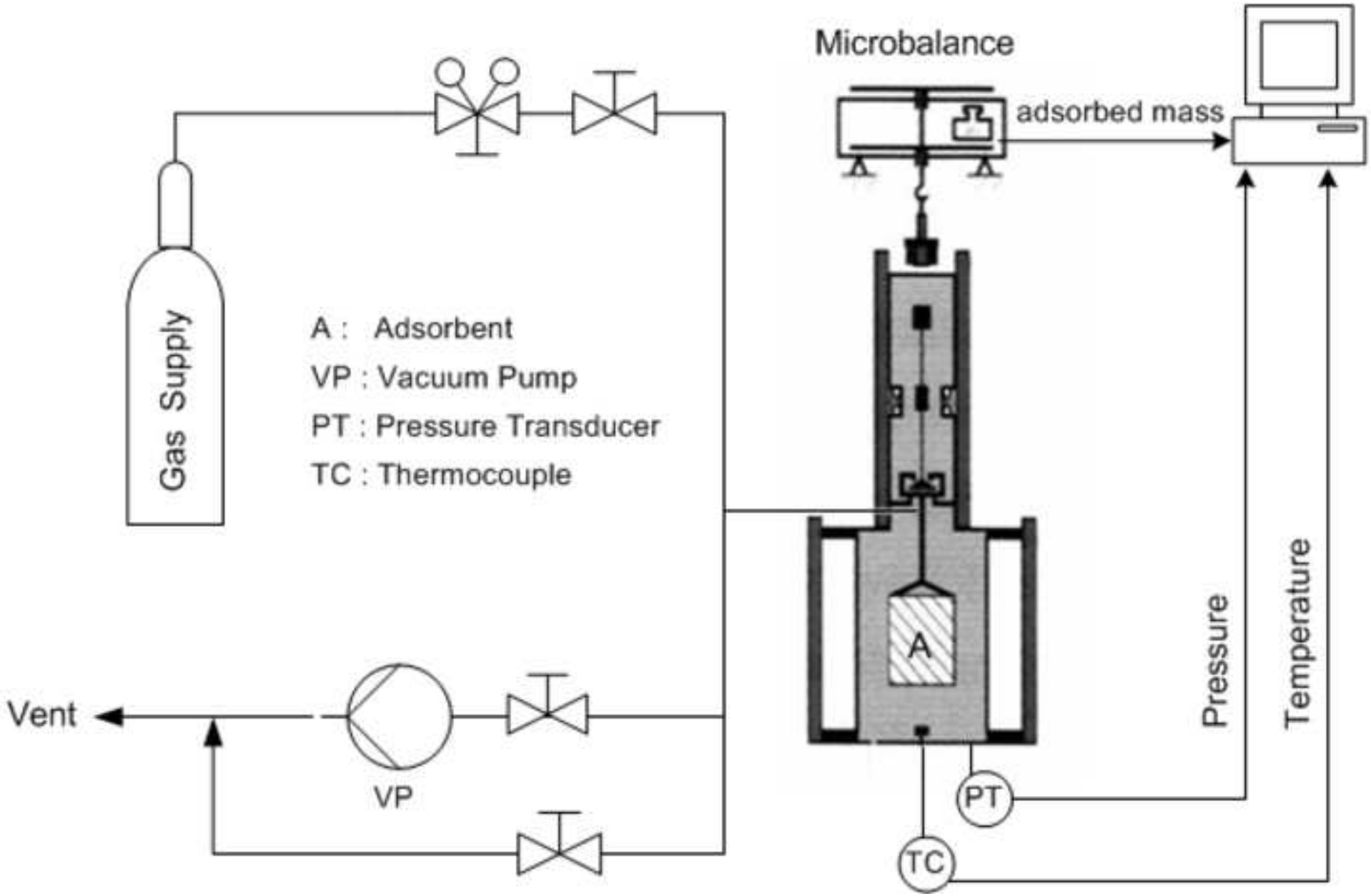

Figure3a

Click here to download high resolution image

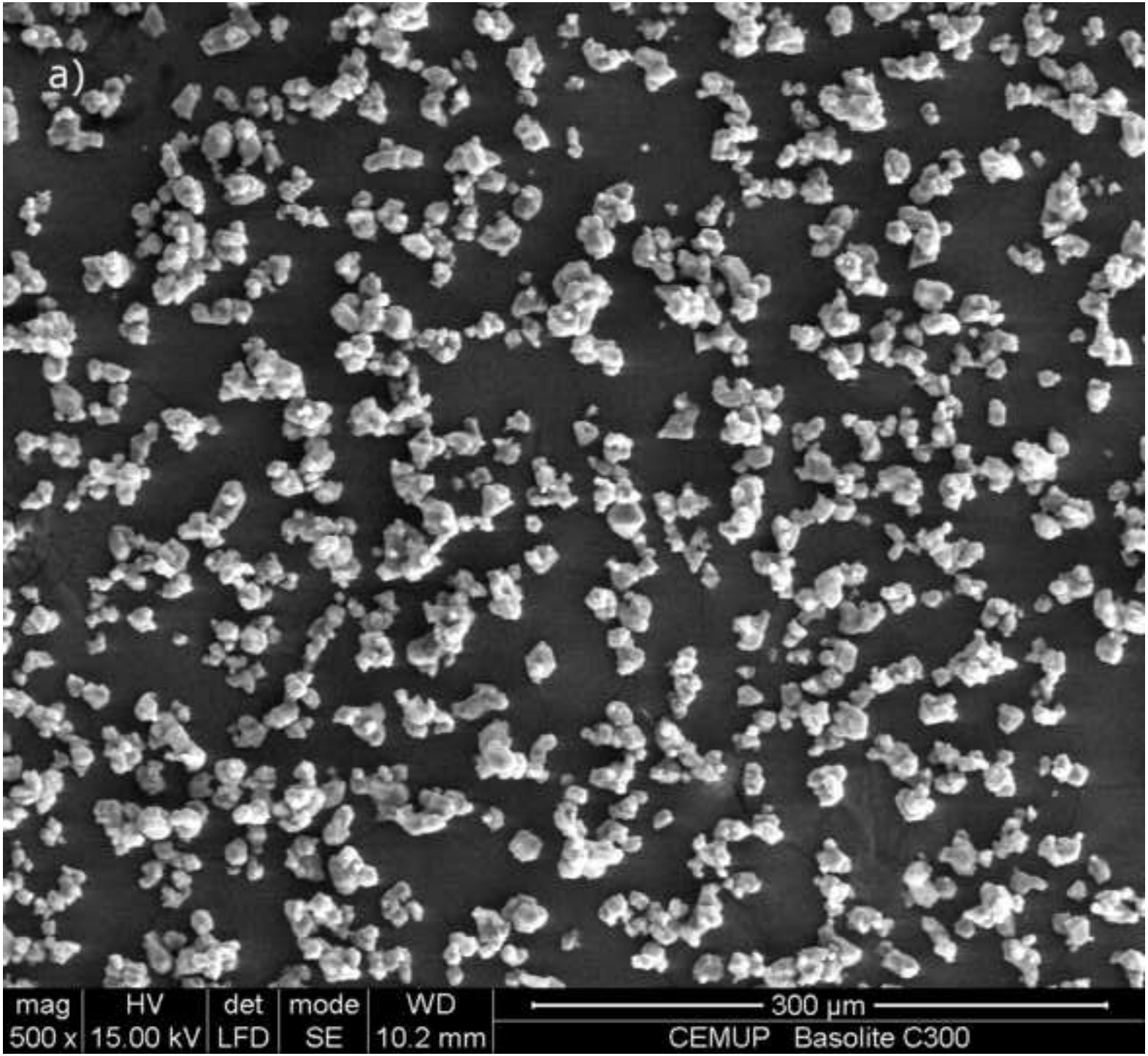

Figure3b

Click here to download high resolution image

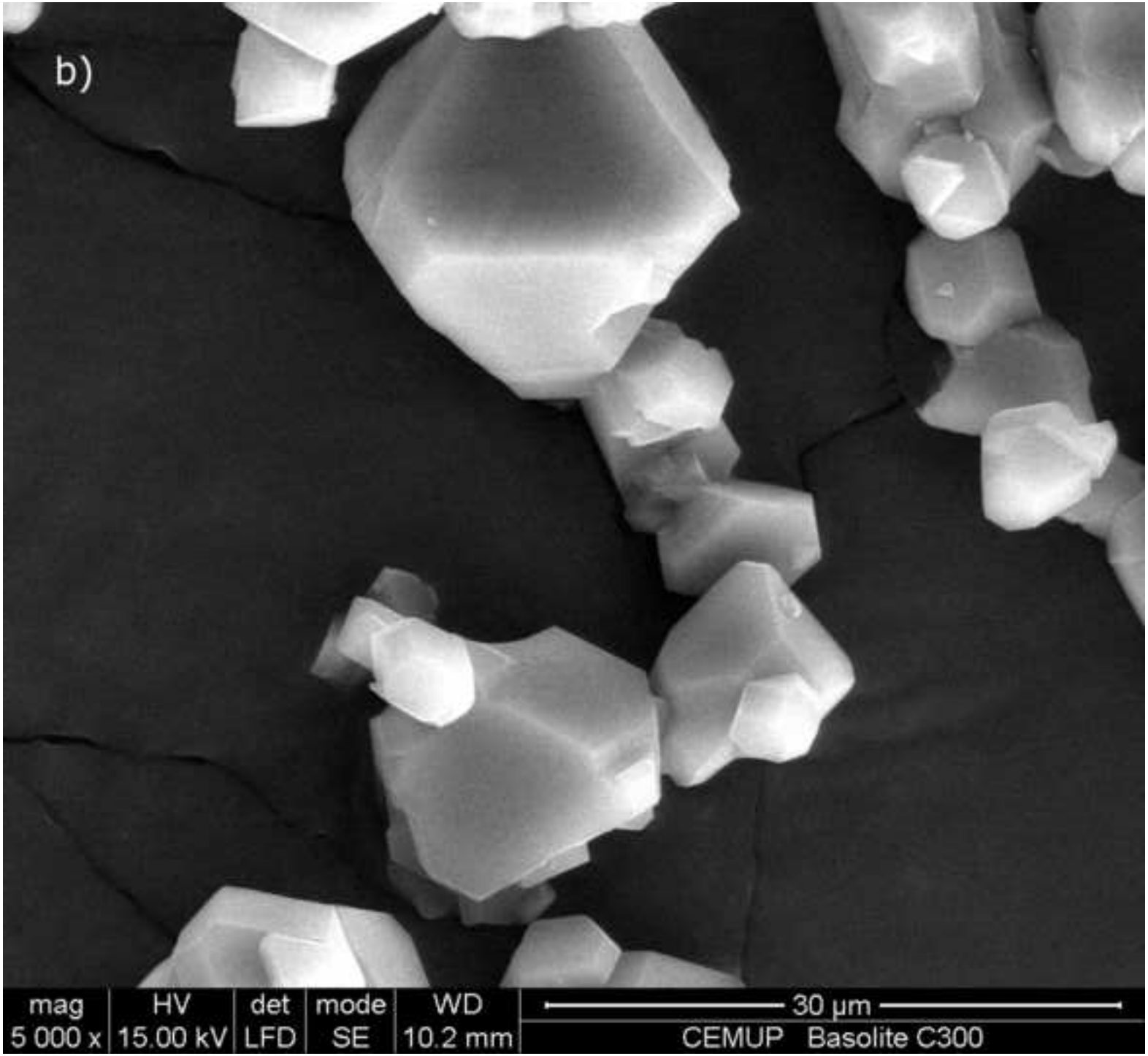

Figure4

Click here to download high resolution image

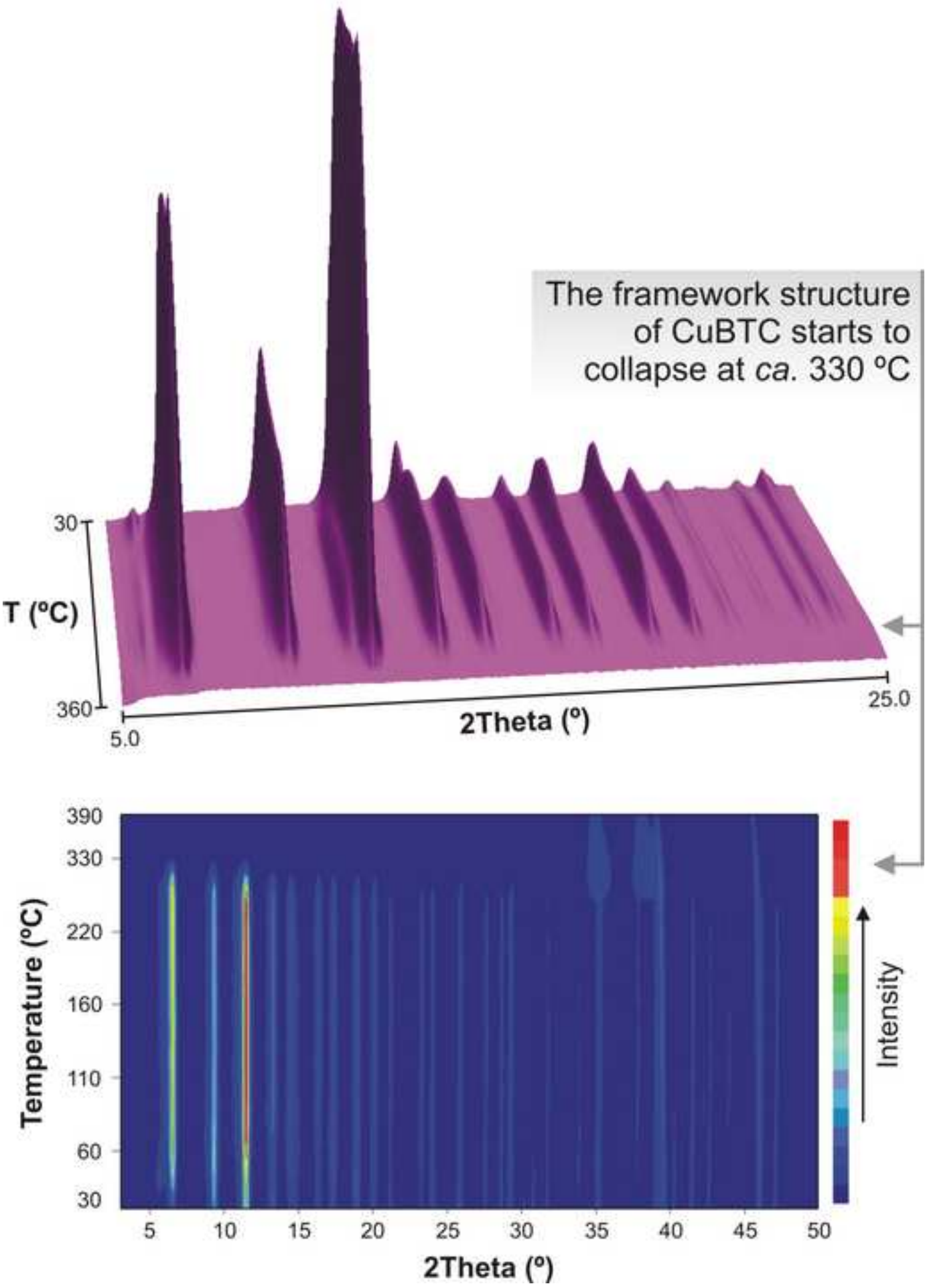

Figure5

Click here to download high resolution image

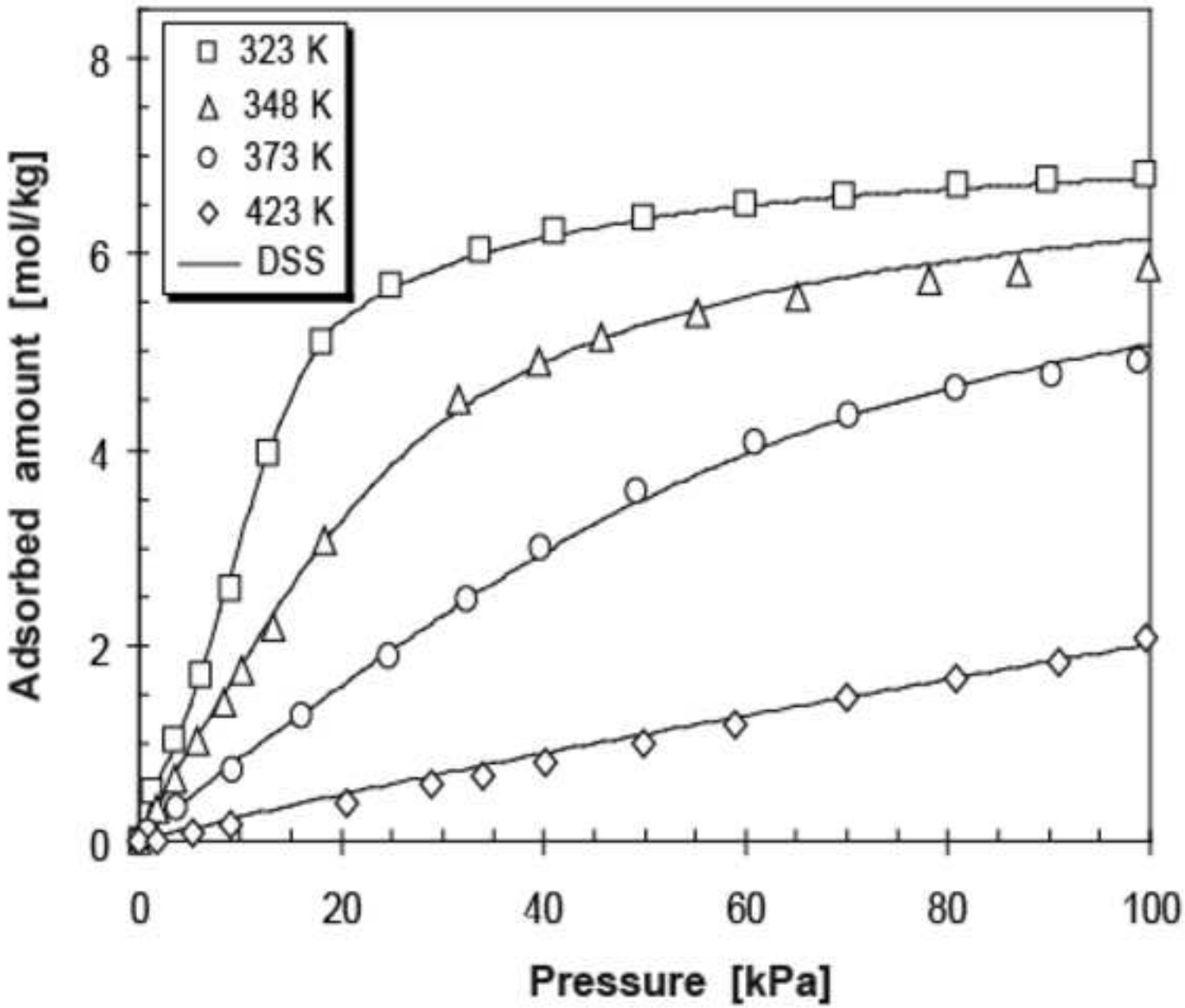

Figure6

Click here to download high resolution image

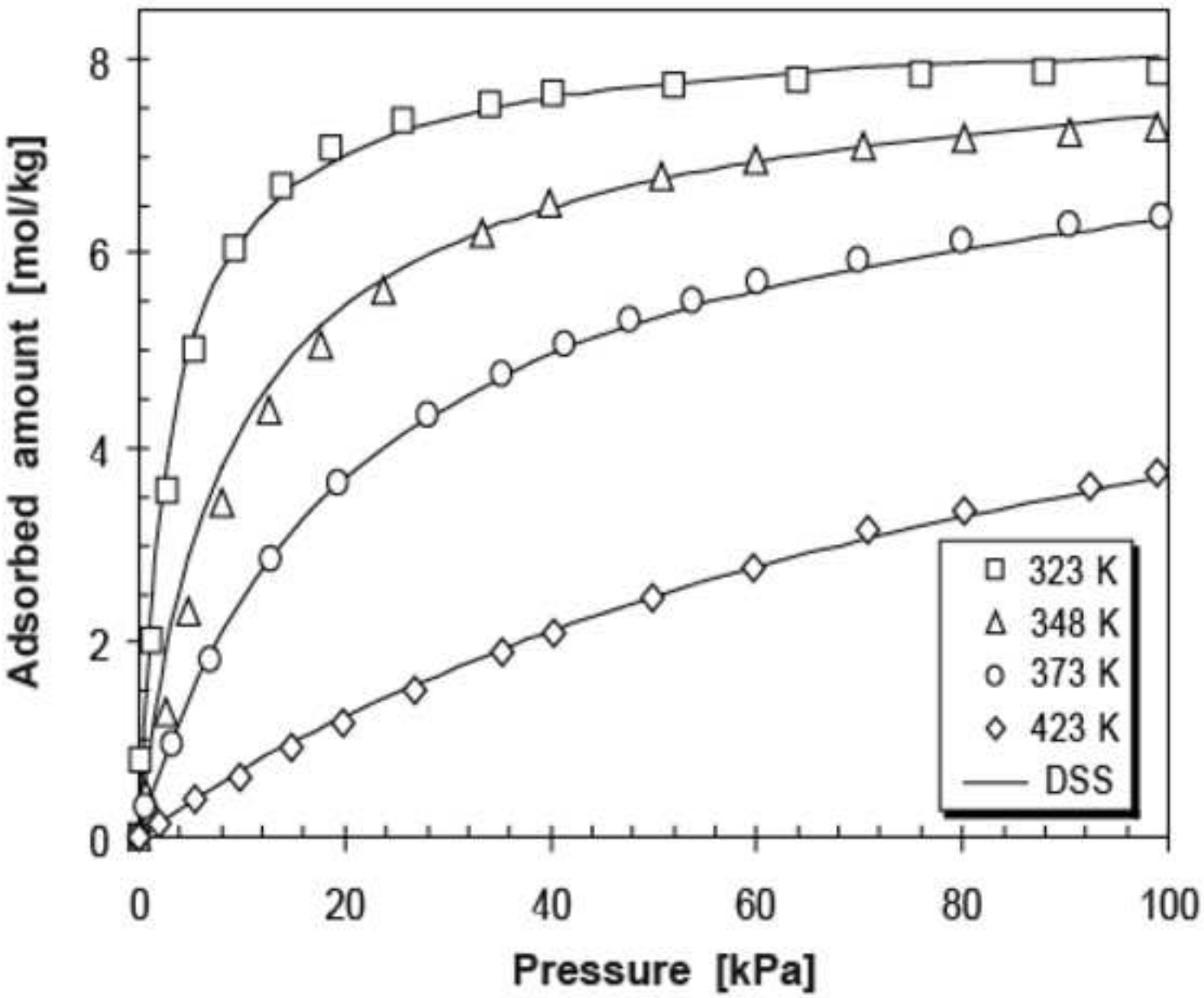

Figure7

Click here to download high resolution image

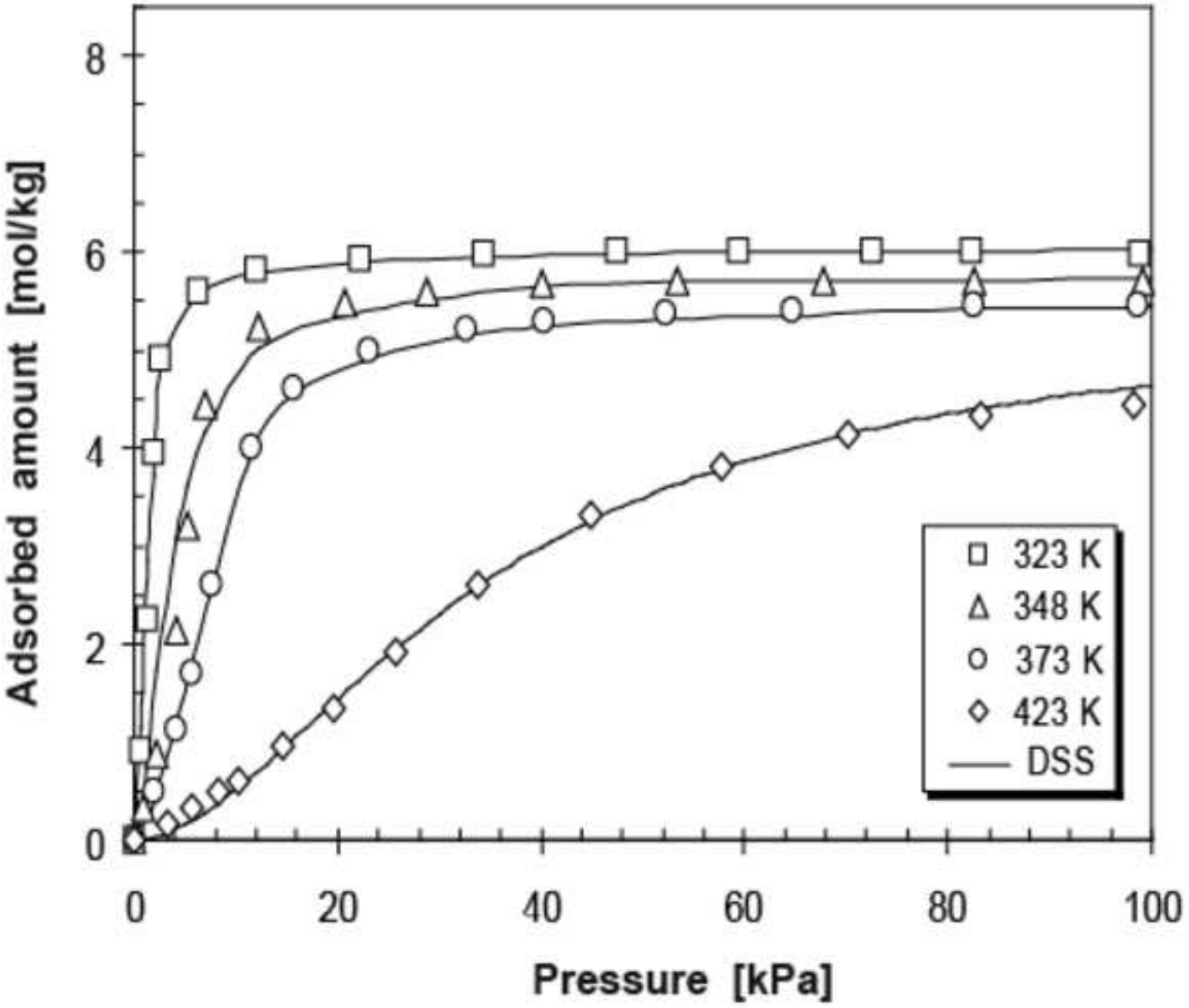

Figure8
Click here to download high resolution image

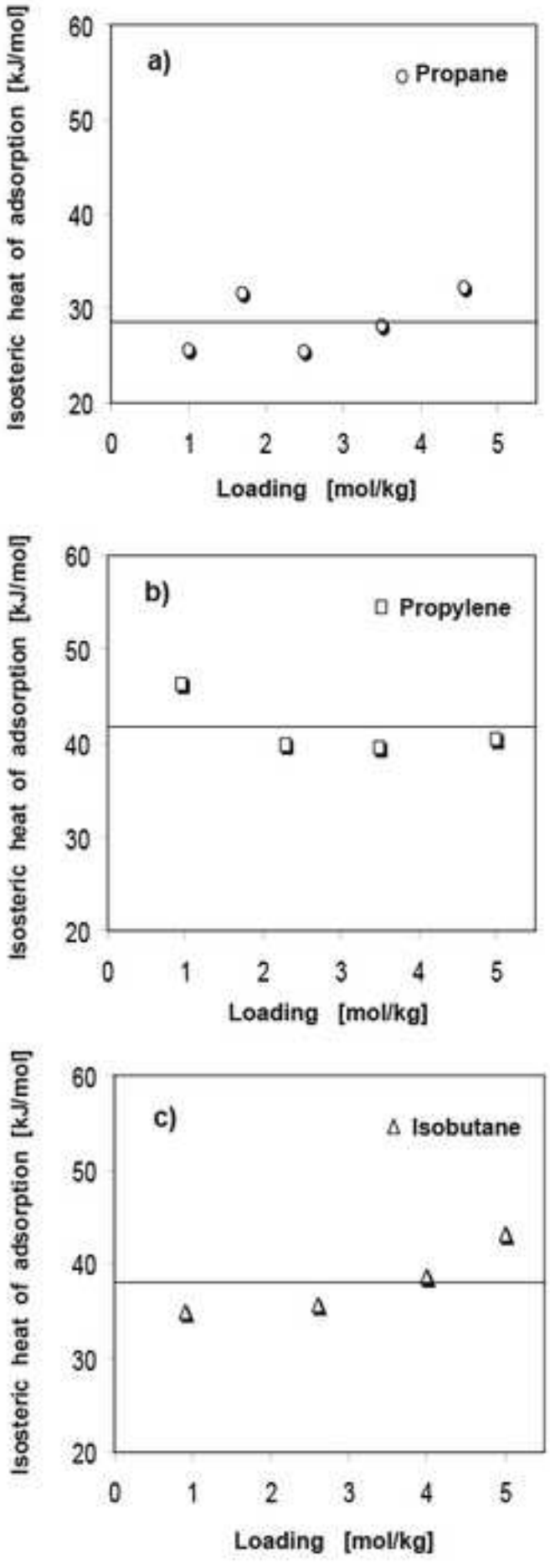

Figure9

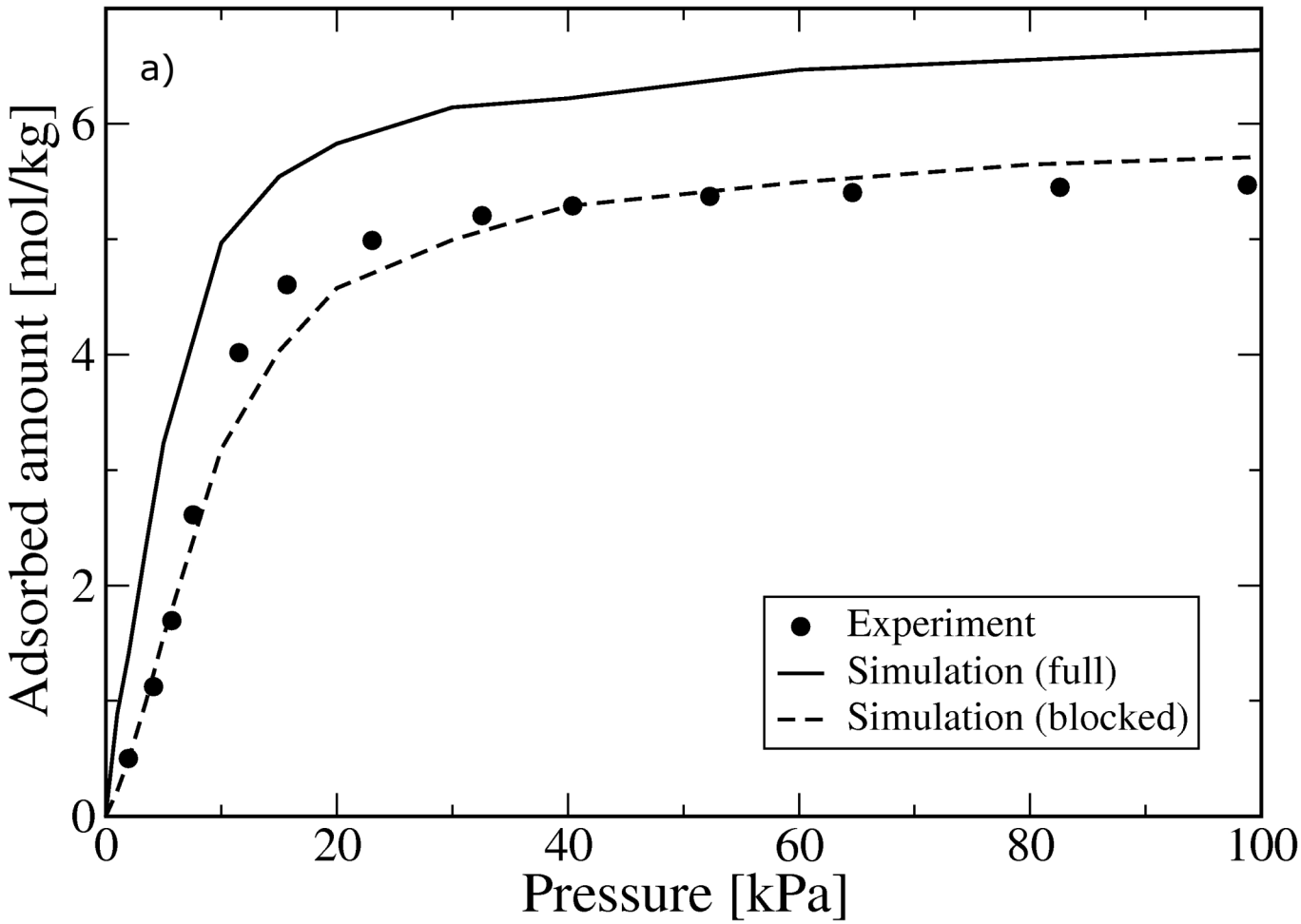
a)
Adsorbed amount [mol/kg]
Pressure [kPa]
0
2
4
6
0
20
40
60
80
100
Experiment
Simulation (full)
Simulation (blocked)

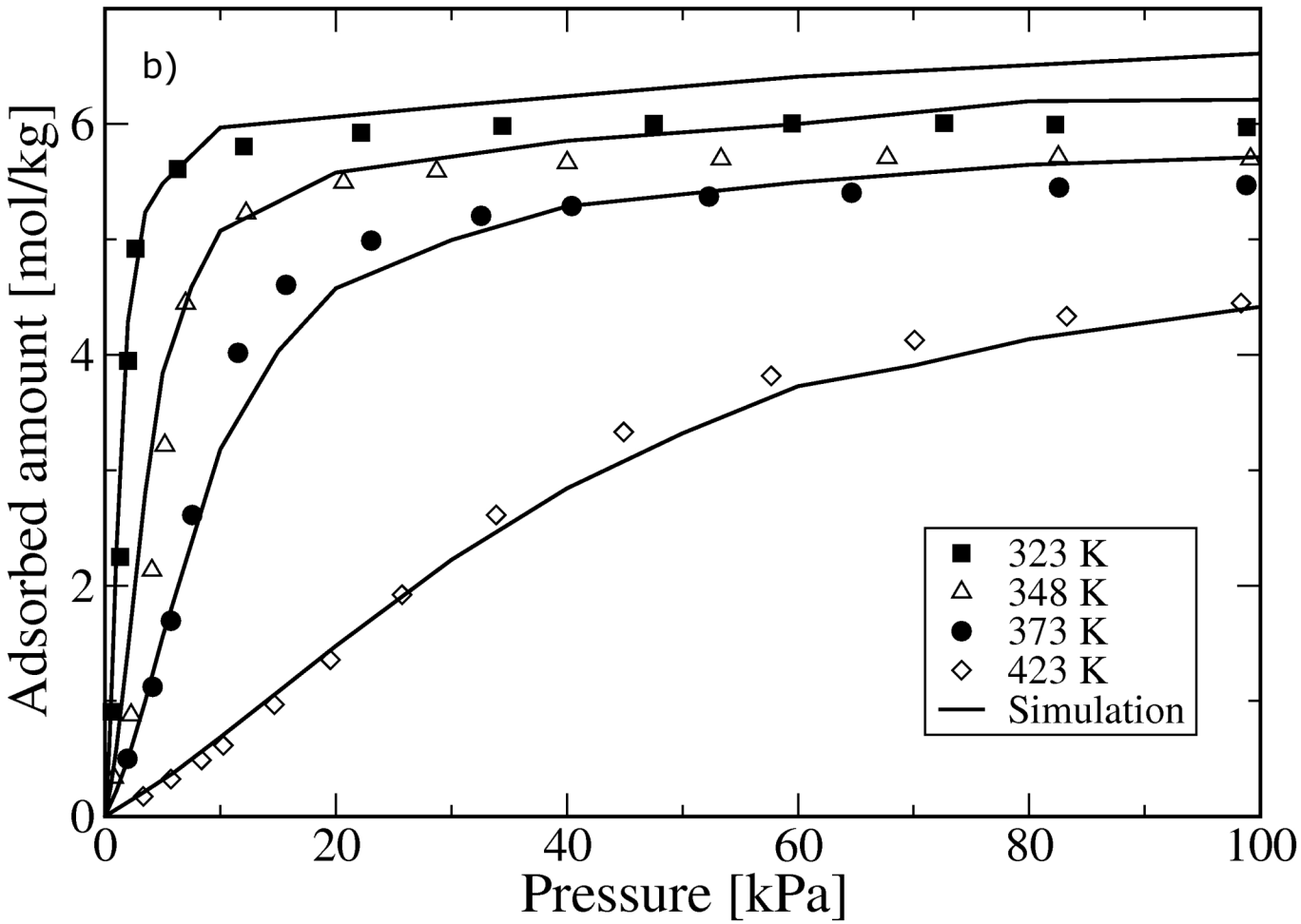
b)
Adsorbed amount [mol/kg]
Pressure [kPa]
0
2
4
6
0
20
40
60
80
100
323 K
348 K
373 K
423 K
Simulation

Figure10

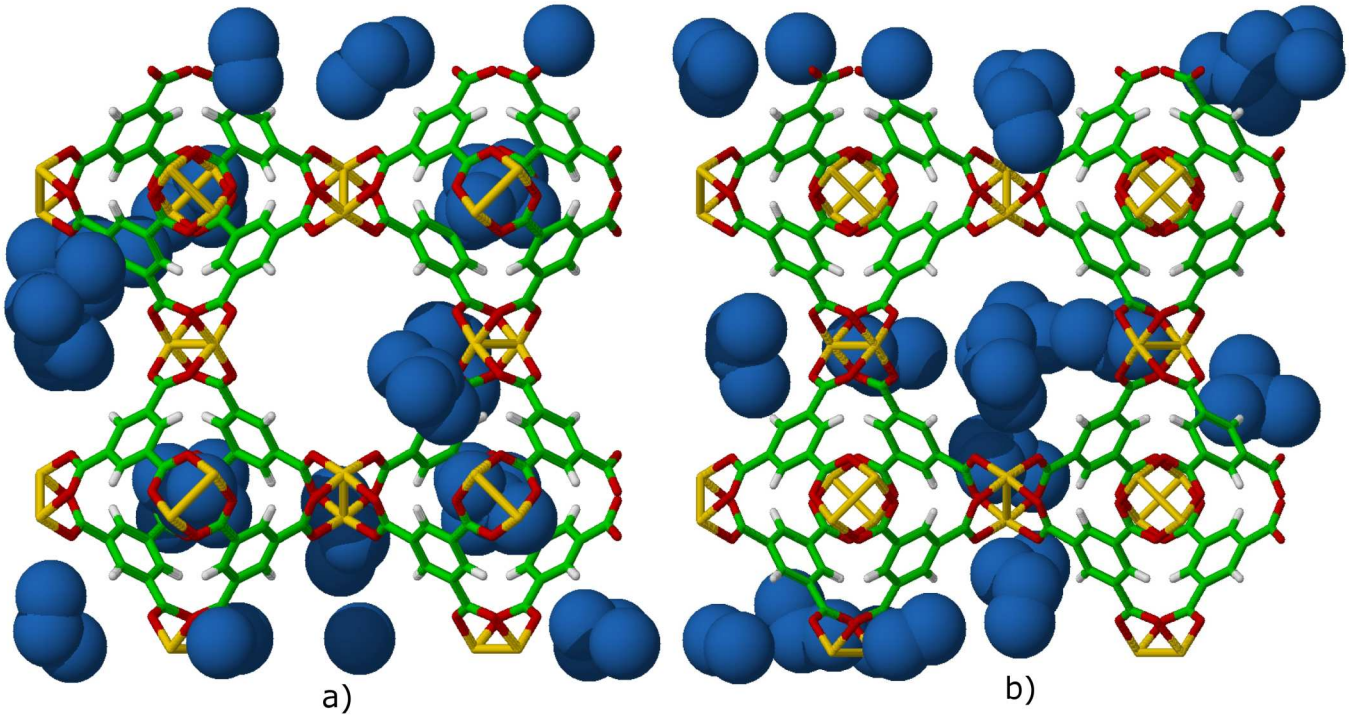

Figure11

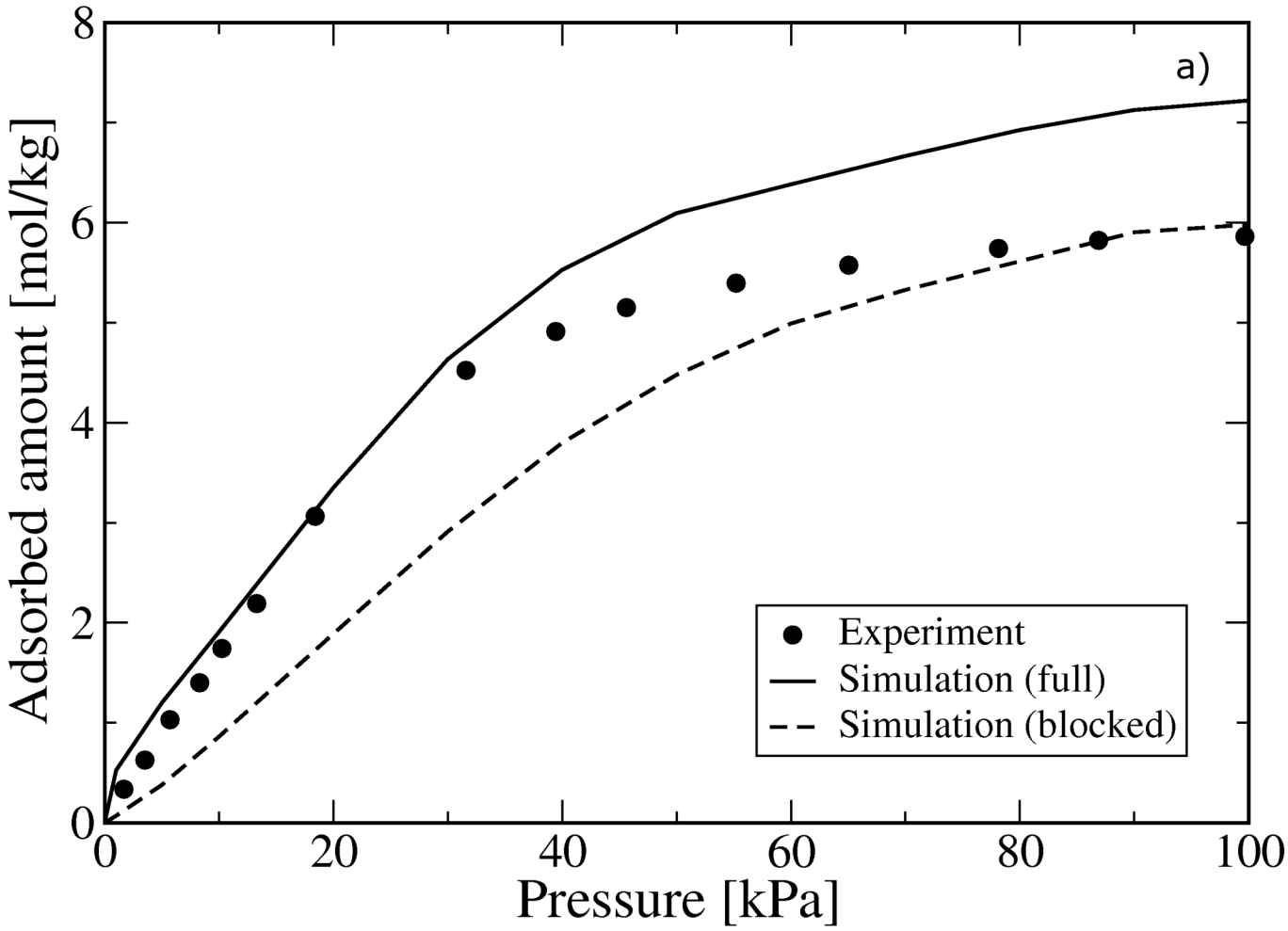
a)
Adsorbed amount [mol/kg]
Pressure [kPa]
Experiment
Simulation (full)
Simulation (blocked)
0
2
4
6
8
0
20
40
60
80
100

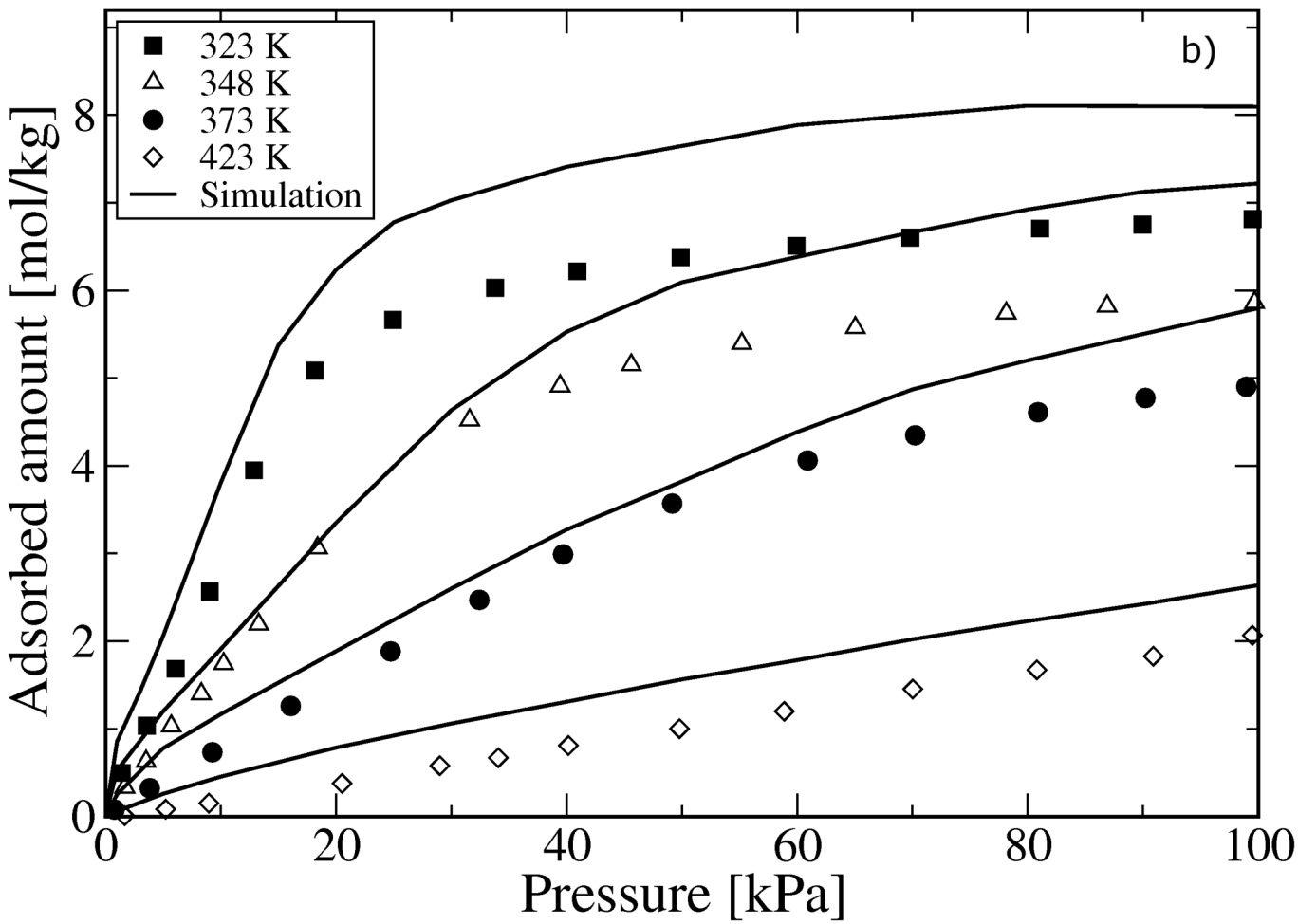
b)
323 K
348 K
373 K
423 K
Simulation
Adsorbed amount [mol/kg]
Pressure [kPa]
0
2
4
6
8
0
20
40
60
80
100

Figure12

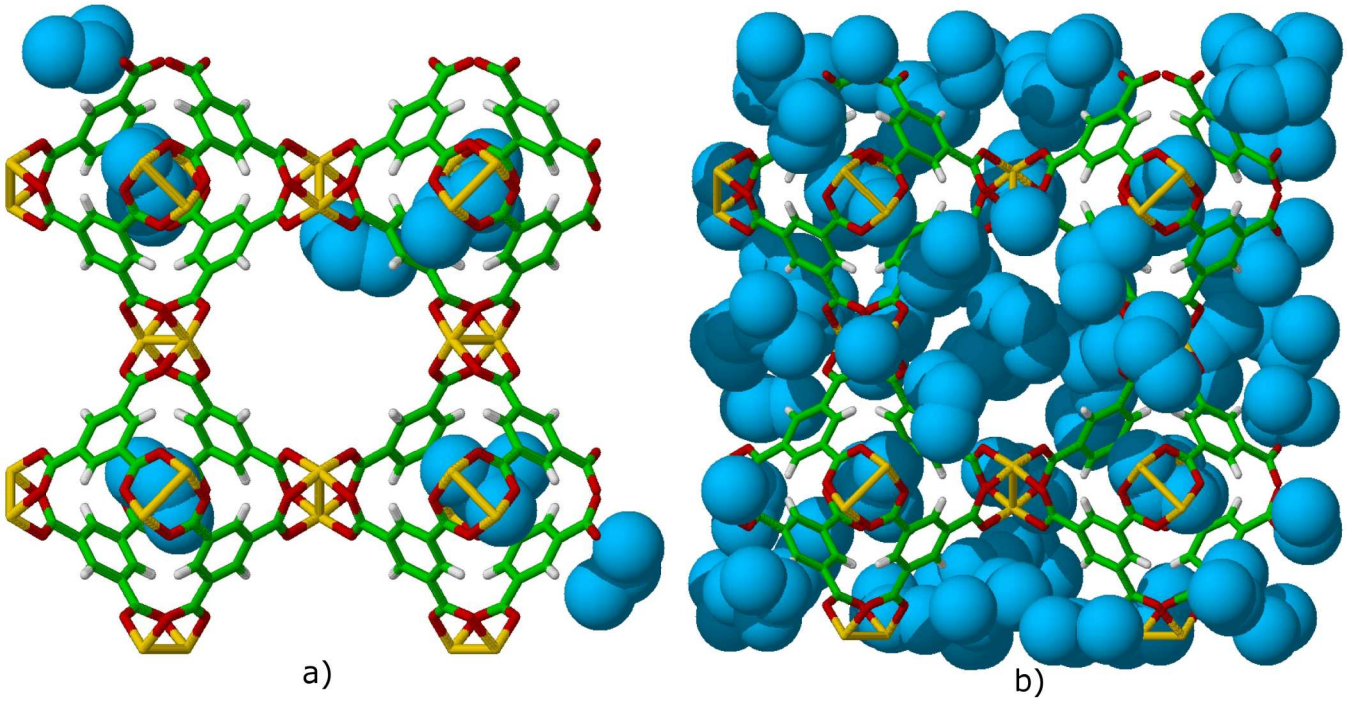

Figure13

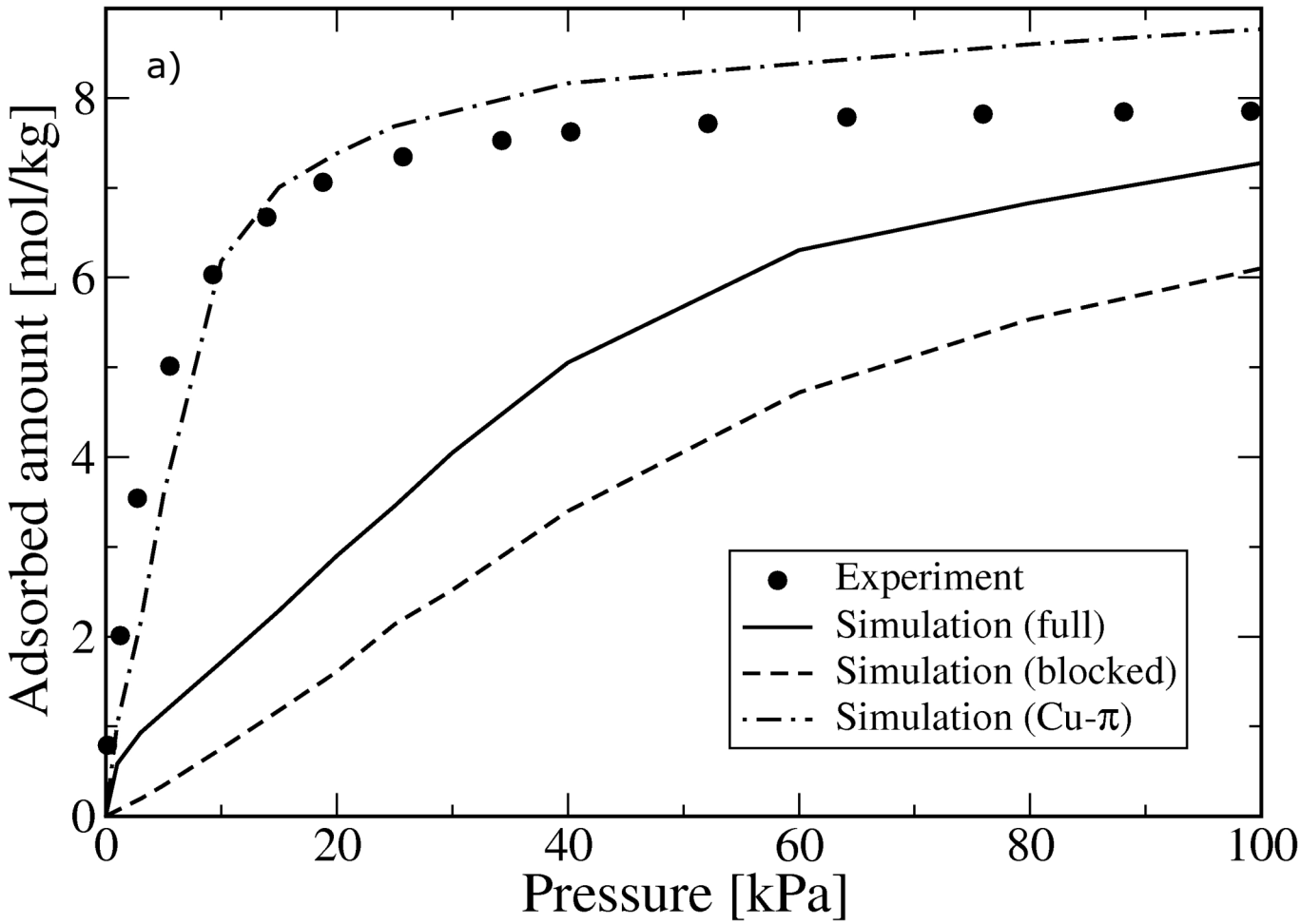
a)
Adsorbed amount [mol/kg]
Pressure [kPa]
Experiment
Simulation (full)
Simulation (blocked)
Simulation (Cu-π)

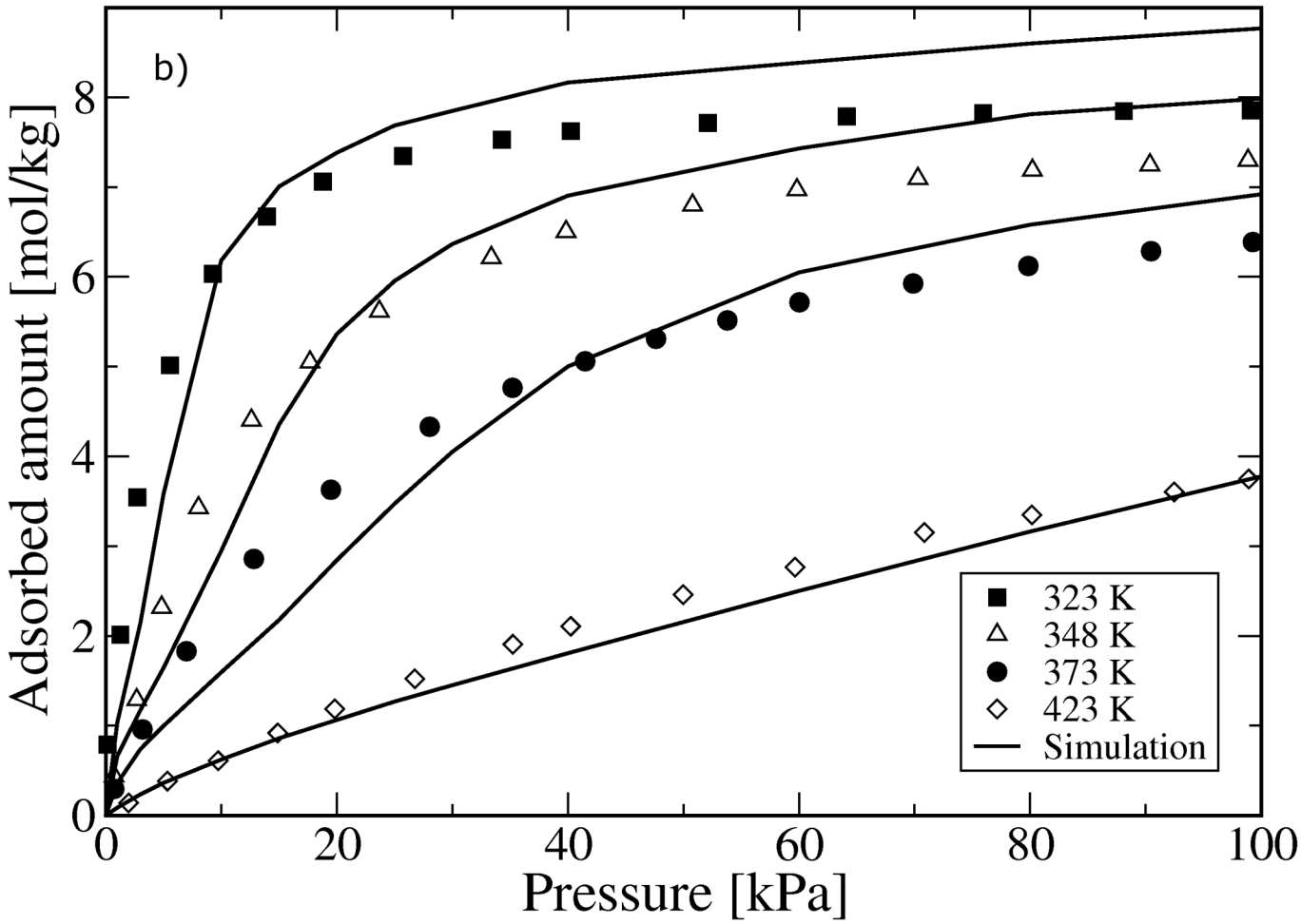
b)
Adsorbed amount [mol/kg]
Pressure [kPa]
323 K
348 K
373 K
423 K
Simulation

Figure14

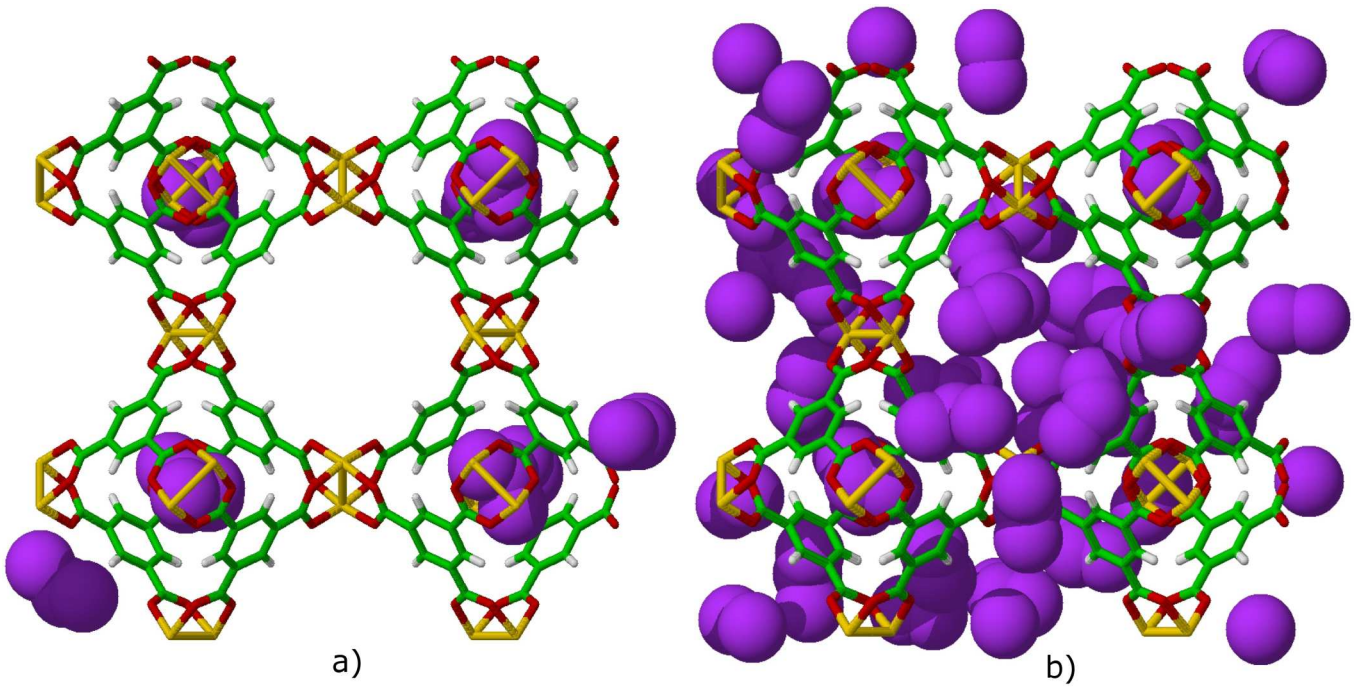

Figure15
Click here to download high resolution image

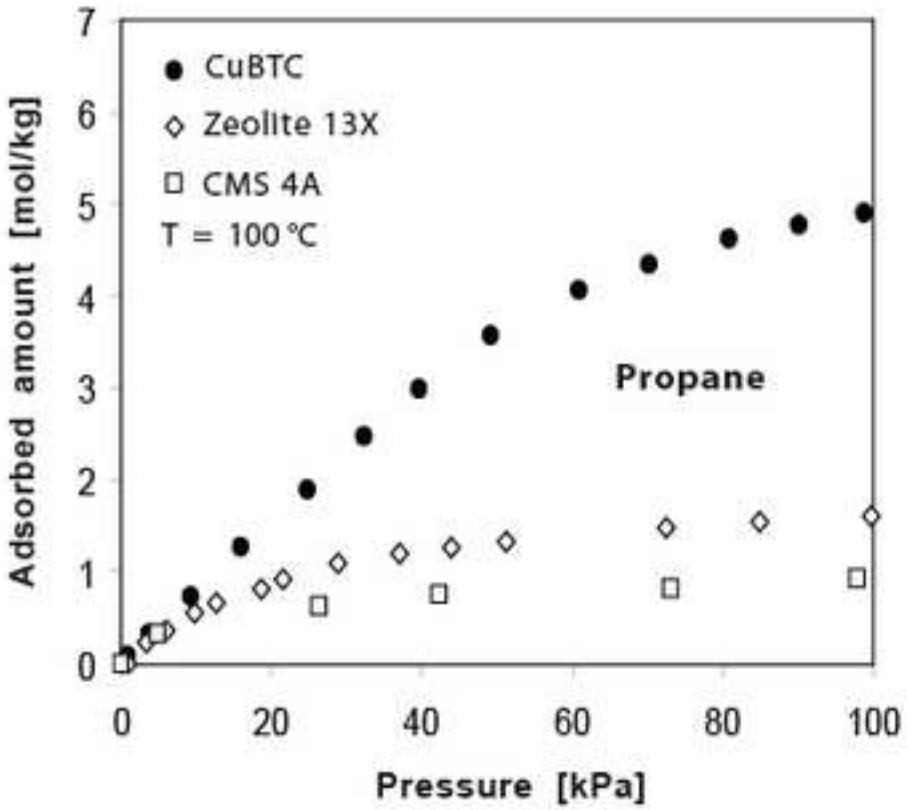

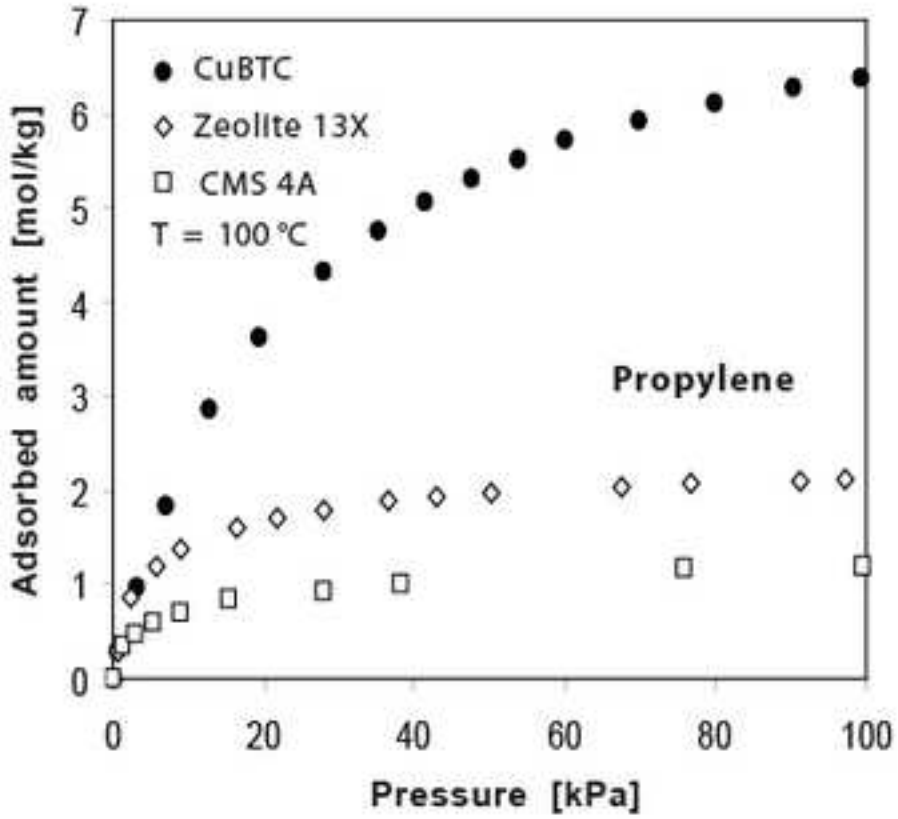

Figure16
Click here to download high resolution image

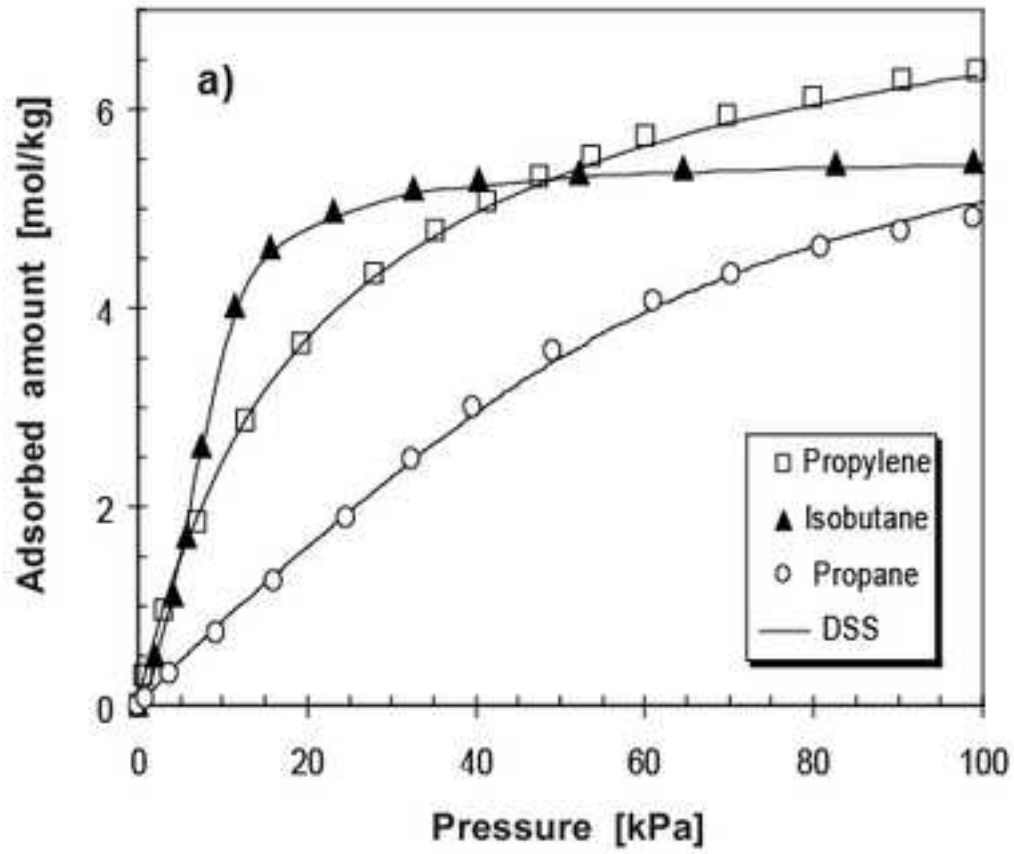

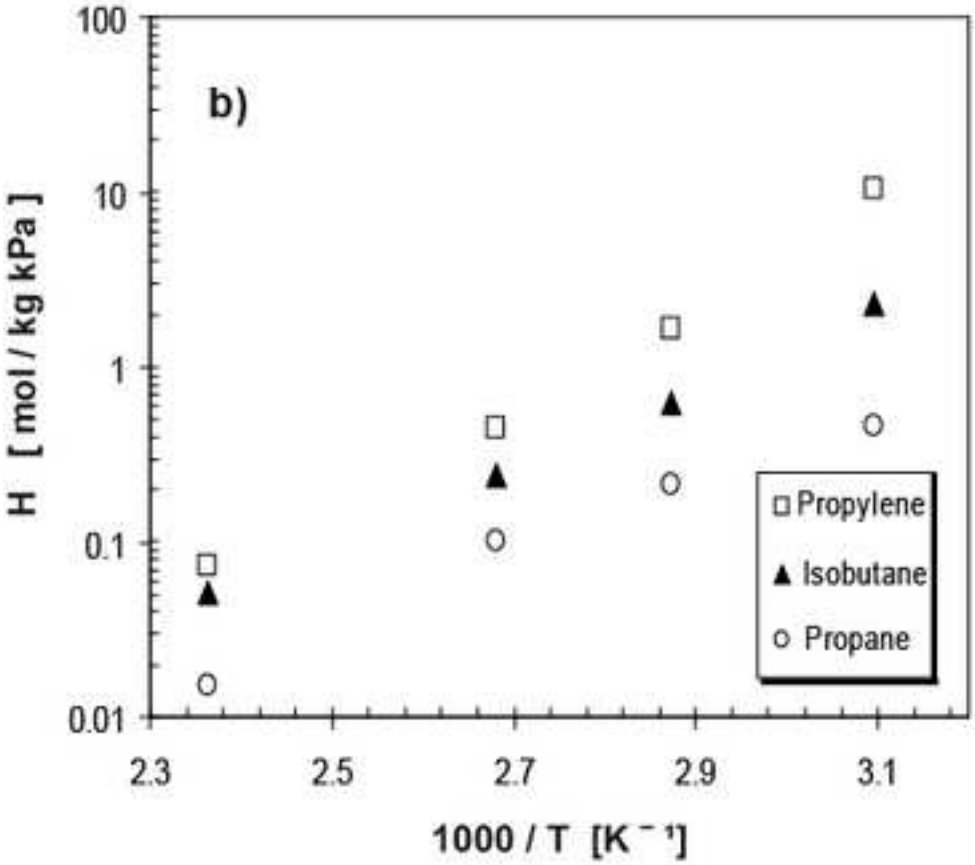

Supplementary Material

Click here to download Supplementary Material: Jorge_SuppMaterial.doc